AD-A059 783 TENNESSEE UNIV SPACE INST TULLAHOMA F/G 20/4
MISSILE VORTEX WAKE MEASUREMENTS.(U)
AUG 78 K E HARWELL, W M FARMER DAAG29-77-G-0107
UNCLASSIFIED ARO-14921.1-A-E NL

| OF |
ADA
059783

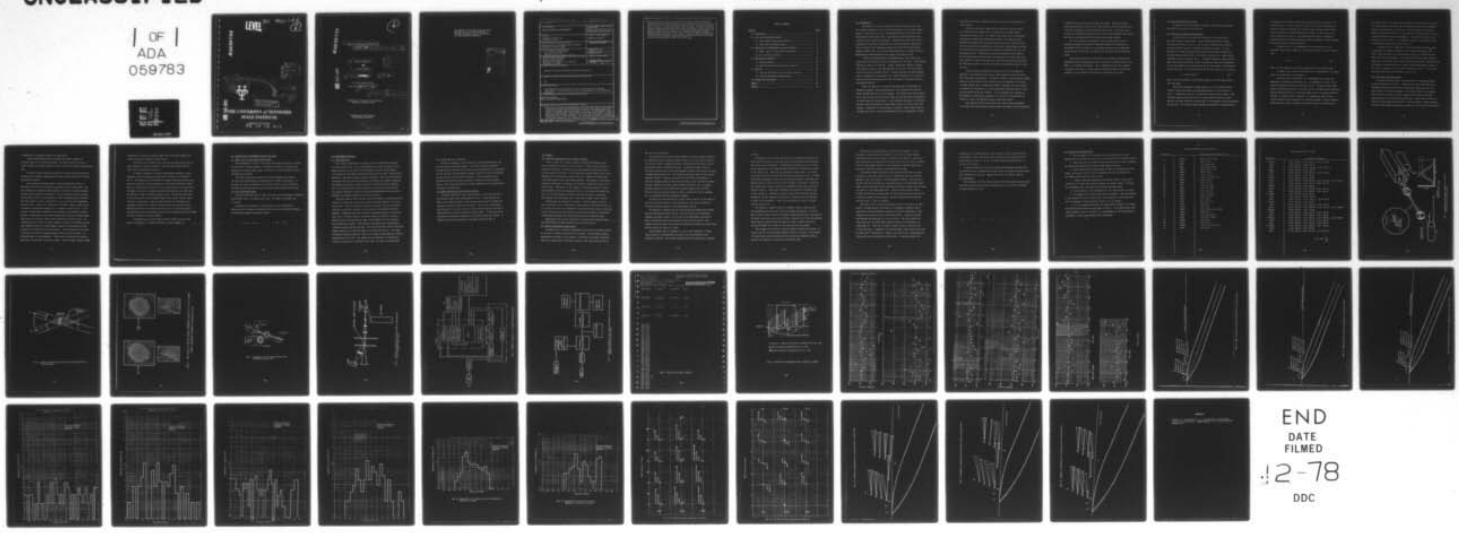

END
DATE
FILMED
12-78
DDC

ARO 14921.1-A-E

LEVEL II

(6)

AD A059783

DDC
RECEIVED
OCT 11 1978
F

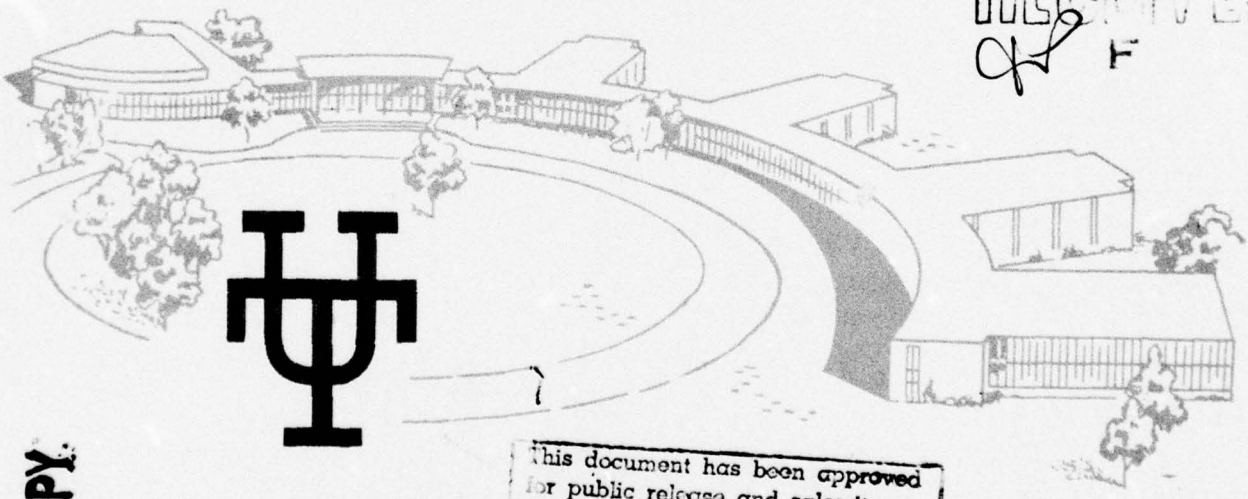

DDC FILE COPY

THE UNIVERSITY of TENNESSEE SPACE INSTITUTE

Tullahoma, Tennessee

6

MISSILE VORTEX WAKE MEASUREMENTS,

FINAL REPORT, 1 May 77 - 30 Jun 78,

Kenneth E. Harwell

W. Michael Farmer

31 Aug [redacted] 78

52p.

U.S. Army Research Office

Grant Number DAAG29-77-G-0107

ARO

14921.1-A-E

University of Tennessee Space Institute
Tullahoma, Tennessee 37388

THE FINDINGS OF THIS REPORT ARE NOT TO BE CONSTRUED AS AN OFFICIAL DEPARTMENT OF THE ARMY POSITION, UNLESS SO DESIGNATED BY OTHER AUTHORIZED DOCUMENTS.

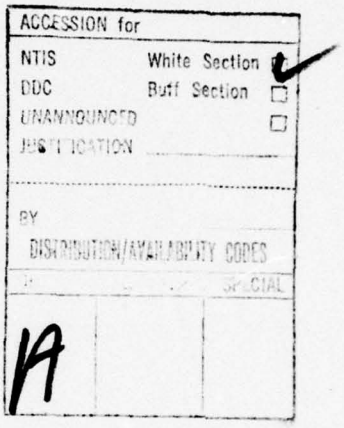

SECURITY CLASSIFICATION OF THIS PAGE (When Data Entered)

REPORT DOCUMENTATION PAGE		READ INSTRUCTIONS BEFORE COMPLETING FORM
1. REPORT NUMBER	2. GOVT ACCESSION NO.	3. RECIPIENT'S CATALOG NUMBER

4. TITLE (and Subtitle) MISSILE VORTEX WAKE MEASUREMENTS	5. TYPE OF REPORT & PERIOD COVERED FINAL REPORT March 1, 1977-June 30, 1978
	6. PERFORMING ORG. REPORT NUMBER
7. AUTHOR(s) Kenneth E. Harwell and W. Michael Farmer	8. CONTRACT OR GRANT NUMBER(s) DAAG29-77-G-0107 new
9. PERFORMING ORGANIZATION NAME AND ADDRESS The University of Tennessee Space Institute Tullahoma, Tennessee 37388	10. PROGRAM ELEMENT, PROJECT, TASK AREA & WORK UNIT NUMBERS
11. CONTROLLING OFFICE NAME AND ADDRESS U. S. Army Research Office Post Office Box 12211 Research Triangle Park, NC 27709	12. REPORT DATE August 31, 1978 13. NUMBER OF PAGES
14. MONITORING AGENCY NAME & ADDRESS(if different from Controlling Office) Office of Naval Research Resident Representative University of Alabama, P. O. Box 1247 Huntsville, AL 35807	15. SECURITY CLASS. (of this report) Unclassified 15a. DECLASSIFICATION/DOWNGRADING SCHEDULE NA

16. DISTRIBUTION STATEMENT (of this Report)

Approved for public release; distribution unlimited.

17. DISTRIBUTION STATEMENT (of the abstract entered in Block 20, if different from Report)

NA

18. SUPPLEMENTARY NOTES

The findings in this report are not to be construed as an official Department of the Army position, unless so designated by other authorized documents.

19. KEY WORDS (Continue on reverse side if necessary and identify by block number)

Missile Aerodynamics
Laser Velocimeter Measurements

20. ABSTRACT (Continue on reverse side if necessary and identify by block number)

This report describes the preliminary results obtained using a dual scatter, moving fringe laser velocimeter system to measure the velocity field downstream of a missile body at high angles of attack. The measurements were made in the NASA/Marshall Space Flight Center Bisonic Wind Tunnel. Problems associated with excessive amounts of oil in the flow prevented a complete characterization of the flow field. Two components of velocity were measured in two planes downstream of the missile nose at an angle of attack of 19.5°.

(Over)

DD FORM 1 JAN 73 1473 EDITION OF 1 NOV 65 IS OBSOLETE

Unclassified

SECURITY CLASSIFICATION OF THIS PAGE (When Data Entered)

The mean velocity, turbulent intensity and kurtosis of the probability density distribution were determined at 45 spatial locations. The mean flow velocity of the wind tunnel freestream was found to oscillate about the mean flow with a time period between 3 and 4 seconds. The mean horizontal velocity component did not vary appreciably (less than 1 ft/sec out of 300 ft/sec), but the vertical component of velocity exhibited both positive and negative components in the vortex flow. Velocity histograms and modal velocities were determined at each spatial location. The report describes the UTSI laser velocimeter system and makes recommendations for its future use in characterizing the missile vortex flows.

TABLE OF CONTENTS

1.0 INTRODUCTION

The purpose of the basic research project described in this report was to make measurements of the velocity distribution in flows over missile bodies at high angles of attack. The measurements were to be made in the NASA/Marshall Space Flight Center 7-inch square subsonic/supersonic wind tunnel facility in Huntsville, Alabama. Measurements of the three velocity components, the turbulent intensities and turbulent velocity correlations were to be made in the separating boundary layer and vortex wake regions behind a missile body. The velocity measurements were to be made using the NASA/Marshall Three-Dimensional Laser Doppler Velocimeter System.

It had been anticipated that the NASA/Marshall 7-inch square wind tunnel would be available as soon as the project was initiated. Unfortunately, this did not prove to be the case. Several months were required to obtain final official approval from NASA management to use the 7-inch wind tunnel and the 3-D laser velocimeter system. Informal agreement had been obtained prior to submission of the proposal, but formal processing of the request to use the facility was delayed until after the award of the grant by the U.S. Army Research Office.

After the approval of the use of the wind tunnel by University of Tennessee personnel, several modifications to the facility were required before experimental data could be obtained. The modifications were necessary due to the fact that the 7-inch wind tunnel facility had not been operated on an active basis for several years. It was therefore necessary to revitalize the wind tunnel facility and to make several repairs to control valves and systems. In addition, it was necessary to install a water coolant line for the high power laser. Since this modification had to be approved by a NASA

group and the work done by NASA technicians, this led to another delay of several months.

Before the high power laser could be operated in the wind tunnel, a new Safe Operating Procedure for the operation of the Laser Doppler Velocimeter System in the 7" x 7" Bisonic Wind Tunnel had to be developed and approved by NASA Safety and Medical Officers. The approved safety regulations required that floor-to-ceiling partitions be installed around the test section and instrumentation, that special warning lights and signs be installed and that special locks be installed to prohibit entry by unauthorized persons. In addition, special eye examinations were required for all UTSI personnel involved with the operation of the high power laser. Final approval to operate the high power LDV system was finally granted and the UTSI group was able to operate the system in June 1978—a delay of about one year.

During a detailed inspection in the Fall of 1977 of the NASA LDV apparatus it was discovered that several items required to make the system fully operational were missing. In addition, several of the electronic systems cables and units would have to be replaced and to be checked out in detail. It became apparent that a considerable number of manhours would be required to bring the LDV system back to a fully operational condition where it could be used by UTSI faculty and students. It was estimated that a minimum of 120 manhours of professional assistance at a cost of over $3,000 would be required to return the NASA LDV system to operational status.

The original intent of the project was to make timely measurements in the NASA wind tunnel facility using the NASA LDV system since The University

of Tennessee did not have an operational LDV system. These measurements and data would provide the basis for a more extensive research program using a new laser velocimeter system being developed at UTSI. It had been anticipated that the NASA LDV system would be used for approximately twelve months and then the new improved UTSI LDV system would become available.

Due to the delays in being able to use the NASA facility and the problems associated with making the NASA LDV system fully operational, it was decided that UTSI should use the new UTSI LDV system in the NASA wind tunnel instead of investing time and money to refurbish the older NASA LDV system.

This report describes the new UTSI Laser Velocimeter System and the preliminary velocity measurements made in the wake of a missile model in the NASA 7" x 7" Bisonic Wind Tunnel. Due to limited funds and time available to complete the project, the data were not extensive enough to provide new insights into the formation and history of the missile vortex wake.

2.0 UTSI LASER VELOCIMETER SYSTEM

A discussion of the UTSI Laser Velocimeter System and its operating principles are presented in this section.

2.1 Laser Doppler Velocimeter Principles

A brief outline of the operating principles for the UTSI Laser Velocimeter System is given here. A more complete description is given by Farmer and Hornkohl in Ref. 1. The UTSI Laser Doppler System utilizes the so-called dual scatter or differential Doppler technique. In this technique, two equal intensity, well-collimated laser beams (created from the same laser as shown in Fig. 1) are made to intersect at a common origin (geometric center) as shown in Fig. 2. A Huygen's diagram of the wavefronts shows that planar interference fringes are generated which are perpendicular to the plane defined by the beam centerlines and are parallel to the bisector between the beams. The distance between the periodic fringes, δ, is given by

$$\delta = \lambda/[2\sin(\alpha/2)] \qquad (2.1)$$

where λ is the wavelength of the coherent light and α is the angle between the laser beams.

The planar interference fringes appear as a set of bright and dark fringes in space (as shown by the photomicrographs in the top portion of Fig. 3). Essentially, one has a "picket fence" scale set up in space. When a particle with diameter less than the fringe spacing crosses the fringe pattern, the light scattered is proportional to the observable flux illuminating the particle. The scattered light intensity as measured by a photomultiplier

is displayed on the storage oscilloscope record as shown in the lower left portion of Fig. 3. If the particle is larger than the fringe spacing, the particle is always illuminated such that the signal intensity never decays to zero so that the resulting photomultiplier output is that shown in the lower right portion of Fig. 3. The photomultiplier output is temporally periodic because the scattering particle moves with constant velocity through a spatially periodic incident intensity.

As shown in Fig. 1, the measurement of the time period τ of the scattered light flux is related to the particle velocity, v, by the relationship

$$v = \delta/\tau \tag{2.2}$$

where v is the component of velocity perpendicular to the fringe planes.

In summary, the velocity is determined from a measurement of the signal period (or equivalently, the frequency).

As can be noted from Equation 2.2, a measurement of τ in the time domain has a directional uncertainty, i.e., the direction of travel of the particle through the fringes is uncertain by 180°. In high turbulent flows where the velocity direction is not known a'priori, the directional uncertainty must be removed by the use of ultrasonic Bragg cells or rotating diffraction gratings to frequency shift a portion of the transmitted light so that a carrier frequency can be generated for the Doppler signal. Doppler frequency shifts about the carrier frequency can then be related to the direction of

the velocity vector. The Bragg cell velocimeter developed by UTSI personnel is a self-aligning system which does not require precise mirror alignments which are quite sensitive to vibration. The UTSI system can measure two velocity components (eventually, it will be able to provide three) using only a single photodetector for both components. A complete description of the technique is given in Ref. 1. A schematic diagram of a LDV system using a two-dimensional Bragg cell is given in Fig. 4.

As shown in Fig. 4, light from a laser operating in the TEM_{ooq} mode is beam split and frequency shifted by the two-dimensional Bragg cell. A lens is used in front of the two-dimensional Bragg cell to make the beams focus and cross simultaneously. Light scattered from the region where the beams cross is collected with a lens system and focused onto a photomultiplier. The signal is then processed by the signal conditioning system to yield the two velocity components (in the X and Y directions in Fig. 4). The signal processing electronics are described in Section 2.2.

2.2 UTSI Laser Velocimeter System

The UTSI Laser Velocimeter (LV) System used for these measurements is shown schematically in Fig. 5. Light from the laser was folded into a 2-D Bragg Cell beam splitter which provided both a beam split and a frequency shift for the incident beams. As described earlier, the frequency shift is used to provide a carrier frequency which allows a particular velocity vector to be identified electronically. Relay lenses focused the beam set to the desired test location in the wind tunnel. Light scattered from this region (probe volume) was collected by a F/9 receiver lens centered

12 degrees off the bisector between the laser beams.

An EMI 9781R photomultiplier tube (PMT) was used to convert the scattered light into an electrical signal. An aperture placed in front of the PMT limited the geometric depth of field of the probe volume to approximately 7-mm.

The entire optical system was mounted on a large traverse system which provided three orthogonal adjustments for probe volume position with 25 micron positional resolution.

The LV signal processing system is shown schematically in Fig. 6. The signal from the PMT is divided and amplified into two signal paths. One path contains the sinusoidal signal component (AC) while the second contains the mean signal component (or pedestal). The AC component enters the system microprocessor labeled S3-PA (Spectrum of Sizes and Speeds-Particle Analyzer) where the signal is tested to determine if it is less than some programmable aperiodic value. This test is conducted if the signal contains enough cycles to generate a measurement attempt (i.e., it passes a precount test). If the precount and aperiodicity conditions are satisfied, the visibility processor performs a measurement and the S3-PA microprocessor obtains an average signal time period for two preset signal cycles (long count and short count). The visibility processor (used to obtain parameters necessary to determine particle size) obtains a measure of the mean signal intensity by integrating the mean component of the signal from the preamplifier. The AC component of the signal is filtered to remove any remaining pedestal and full wave rectified. The rectified signal is then integrated. These results, along with the long and short count time periods are stored in memory. When the memory contains enough

measurements to satisfy a prechosen sample size, the system computes the various output data parameters shown in Fig. 6.

Calibration of the system with a precision oscillator shows that for large samples, the system is capable of computing mean signal period to better than 100 picosecond resolution.

A schematic diagram of the signal conditioning electronics, signal processor, and data acquisition system used for these tests is shown in Fig. 7. The signal from the PMT enters the signal conditioning electronics where the respective velocity components are identified, amplified, heterodyned to a lower carrier frequency and then passed through a low pass filter. The signal then enters the signal processor which measures the signal time and performs a number of signal validation tests. The measured time period is then entered into a small computer memory which records a preset number of velocity measurements. When the required number of measurements are completed, the mean flow velocity, turbulent intensity, kurtosis and probability distribution are computed and printed out in a hard copy format. The individual velocity measurements used in these computations can be recorded as often as required for later analysis.

A reproduction of a typical page of printer output for one of the tests in the NASA 7" x 7" Bisonic Wind Tunnel is given in Fig. 8.

3.0 DESCRIPTION OF EXPERIMENTAL FACILITY AND MODEL

3.1 NASA 7 Inch x 7 Inch Bisonic Wind Tunnel

The NASA/Marshall 7 inch x 7 inch Bisonic Wind Tunnel was used to provide the flow about the missile models. The tunnel is capable of providing flow velocities in the Mach number range from 0.35 to 4.5 using a family of interchangeable nozzle blocks.

The tunnel presently processes air from the atmosphere and achieves the test section Mach numbers by exhausting into a large vacuum sphere. In the past, the tunnel utilized dry air, but the air dryer is not attached to the Bisonic Wind Tunnel and is used with another NASA supersonic wind tunnel.

3.2 U.S. Army Missile Model

The wind tunnel model used in these tests was a 0.8 inch diameter cylindrical missile model with a 1.2 caliber ogive nose. The length of the model was 9.6 inches.

The model was provided by Dr. Donald Spring of the Aeroballistics Directorate of the Advanced Technology Laboratory of the Army Missile Research and Development Command at Redstone Arsenal.

4.0 EXPERIMENTAL PROCEDURE

4.1 Data Acquisition

After initial shakedown of the system, the data acquisition proceeded in the following manner. Due to the availability of only one channel of the signal processor at the time of the measurements, only the 15 MHz channel of the Bragg cell and signal conditioning electronics was used. During typical operation, a horizontal velocity component (parallel to the tunnel centerline) was measured and then the second channel of the Bragg cell (normally operated at 45 MHz) was operated at 15 MHz to obtain the vertical velocity component. Thus, in the velocity data taken, there was no correlation in time for the two measured components so that the resulting two-dimensional velocity vector represents an ensemble average for the mean velocities.

Data were acquired after the wind tunnel was brought to a preset operating condition as determined by the static pressure measured forward of the tunnel test section. When the operating condition was reached, the data acquisition system was instructed to acquire a preset number of measurements (typically 500-900). Immediately after these data were acquired (typically in times less than 1 sec.), the mean velocity, turbulence intensity, kurtosis of the probability density distribution and number of measurements in the calculation were computed and recorded. This sequence was repeated until approximately 2,000 measurements had been obtained. This required between 5 and 10 repetitive samples because of the rejected signals in the acquired data set. This type of sampling procedure allows for tests of the statistics governing the velocity distributions of the flow. For example, is the assumption of constant mean velocity a good one for a particular test point? Or, what is the precision

for a given turbulence intensity?

In order to determine a flow direction, a carrier frequency was used for each velocity component channel. The carrier frequency produced a fictious velocity such that 100 ft/sec from the signal processor corresponed to zero velocity in the horizontal component, while 300 ft/sec corresponded to zero velocity in the vertical component. Velocity magnitudes were determined by subtracting these reference velocities from the measured values. The velocity direction for a given component was then determined by the sign of the difference.

4.2 Model Orientation and Test Point Locations

The model supplied for these tests was placed in the test section at the maximum possible angle (approximately 19.5°). A grid template was made to fit around the model so that all test points could be readily and repeatedly identified relative to the model. After a set of grid points was selected for the tests, the probe volume cross-section was centered on the grid point of interest using the traverse system. In this way, errors resulting from mechanical backlash in the traverse screws was avoided. A sketch of the test grid relative to the model is given in Fig. 9.

5.0 RESULTS

5.1 Velocity Measurements Prior to Model Insertion

Prior to tests with a model in place, preliminary measurements were made at different locations in the test section. These tests were made to evaluate the presence of naturally occurring aerosol particles in the flow and the quality of the flow. It was found that extremely high levels of what appeared to be oil droplets existed in the flow. Sample rates were found to be high enough to avoid most sampling biases. Measurements at the tunnel centerline showed what was thought to be turbulent intensities in the 2 to 3 percent range. Examination of the sequence of data points placed at equal time increments during the acquisition time for a particular run showed that the 2 to 3 percent turbulent intensity level was in reality a relatively slow periodic flow fluctuation with a time period between 3 and 4 seconds.

Experimental data obtained at Position 1 (located slightly above the nose of the model) over a time period of 200 seconds are presented in Fig. 10. It is clear that there are considerable excursions about the mean flow velocity of 167.5 ft/sec and that oscillations in the mean flow present a problem when correlating experimental data from different points at different times.

Measurements near the top and bottom of the wind tunnel indicated that the flow velocity was fairly uniform across the test section.

5.2 Velocity Measurements Behind Model

As shown in Fig. 9, velocity measurements were made in two planes located at 0.5 and 2.25 inches from the nose of the model. At each radial distance, measurements were made at three points: one located in the model centerline plane, one forward (out of the paper relative to the centerline) and one to

the rear of the centerline.

The procedure was to record a given number of velocity component readings into memory and then to perform validation tests on the data before printing out the mean velocity component and then a listing of the individual velocity data that was used to establish the mean. As previously shown in Fig. 8, the signal processor was to store 900 readings in memory, then process allowing a maximum aperiodicity of 5%. Four separate tests were taken at this location (position 5 Back). These data are given below the table of parameters. A velocity (frequency) shift of 100 ft/sec was used, so that the mean horizontal velocity components were 288.6, 288.8, 288.48, and 287.65 with a turbulent intensity between 3.61 and 4.125% and a kurtosis between 4.567 and 5.82. As can be seen from the data listed in Fig. 8, between 565 and 646 readings out of a maximum of 900 were acceptable readings.

The data from the microprocessor output printer (similar to that shown in Fig. 8) was then processed to yield histograms of the velocity components as well as the mean velocity at each measurement location.

The horizontal component data were well-behaved and yielded fairly narrow velocity distributions about the mean. The mean values of the horizontal component are shown in Figs. 11-13 at each of the measurement locations in Plane I (points 3,5,6,7,8) and in Plane II (points 9,10,11,12,13). The largest velocity variation at any point was less than 5 ft/sec out of 290 ft/sec and was usually the order of 1 ft/sec.

The horizontal data at locations 3,5, and 6 were obtained at a tunnel static pressure of 19-mm Hg while the data at all other positions were obtained at 20-mm Hg. All vertical component data were obtained at a pressure

of 20-mm.

In contrast to the relative stability in the horizontal direction, the flow velocity fluctuated a great deal in the vertical direction resulting in very broad velocity histograms. Histograms were prepared for each location, but are presented only for positions 3BCF and 11BCF to illustrate the nature of the complex flow. These data are presented in Figs. 14-19. It is quite clear that the flow in the vertical direction reverses quite often. On these preliminary measurements, there was not sufficient memory to time code each particle burst, so that the time of flow reversals is not known. A table of the various modal vertical velocities was prepared from the data and is presented as Table I. These modal velocities are presented in graphical form in Figs. 20 and 21. Combining the modal vertical velocities with the mean horizontal velocity component at each point a velocity vector in the plane of paper can be determined. These data are presented in Table II and are plotted in Figs. 22-24.

The presence of negative vertical components seems to indicate that the measurements did cross the vortex layer behind the missile. As can be seen in Figs. 20 and 21 there is a definite change between Plane I and Plane II. The modal velocities on the center of Plane I (points 3,5,6,7) are all positive. while there are negative modal velocities at Plane II (points 11,12,13). The same statement can be made for the front and back flow planes.

Even though the data are not complete enough to analyze much further, it appears that the flow is turning toward the model as it should. The presence of several modal vertical velocities (both positive and negative) seems to indicate the shedding of vortices from the missile body.

These data were obtained under very difficult conditions. It was necessary to shut down the wind tunnel to clean the wind tunnel windows which became coated with oil after a very short time interval. Data could only be obtained at a single position on any given run due to the oil problem. The oil on the windows resulted in large amounts of scattered light which resulted in high noise levels in the photomultiplier tube.

Even though the LDV electronics could take sufficient data at a given location in a very short time interval, a considerable amount of time was required to move the system to a new measurement location. This was due to the fact that the LDV mechanical traversing system in the NASA Bisonic Wind Tunnel had not been used in quite some time and required manual force to move the system to a new measurement point. Before the new position could be reached, the PMT noise resulting from the laser light scattered from the oil on the test windows became excessive, thereby necessitating shutting down the wind tunnel to clean the windows.

The source of the oil was not determined prior to the end of the grant period. The NASA Bisonic Wind Tunnel is an atmospheric blowdown type of wind tunnel in which atmospheric pressure air from the atmosphere in flows through the test section into a large vacuum sphere. Valves are located both upstream and downstream of the test section. The valve between the test section and the vacuum sphere should prevent any back migration of vacuum pump oil. There are no internal sources of oil on the inlet side of the wind tunnel. Atmospheric air flows through a large control valve into the wind tunnel plenum section. However, the control valve is hydraulically driven and could be leaking oil into the flow. It would seem that this

explanation is not reasonable due to the excessive loss in oil which should be detectable. Due to the limited time available and the exhaustion of the grant funds, the source of the oil was not definitely established prior to the end of the project.

It had been anticipated that the preliminary measurements program would be followed by a more extensive one at more spatial locations and would include time correlation of the data. However, due to the oil problem, this was not accomplished.

The preliminary data did indicate that the UTSI LDV System was operational and could be used to take velocity measurements in a wind tunnel environment in short intervals of time.

6.0 SUMMARY AND RECOMMENDATIONS

1. The experimental data described in the previous section clearly demonstrated the satisfactory operation of the new UTSI Laser Velocimeter System.

2. Additional data are required before conclusions can be made concerning the vortex flow behind missile bodies at high angles of attack.

3. Before additional LDV measurements are made in the NASA Bisonic Wind Tunnel, the source of the oil must be determined and the oil eliminated or the amount greatly reduced in the air flow.

4. A better traversing system must be devised to permit a more rapid traversal of the laser probe volume throughout the spatial region of interest. It is preferable that this system use an optical scanning system.

5. All data must be time correlated since the flow is highly turbulent.

6. It appears that the wind tunnel flow is nonsteady. This unsteadiness in the incoming flow will strongly affect flow separation on the missile and must be eliminated if good quantitative data are to be obtained.

7. It is recommended that additional measurements be made of the complex flow behind missile bodies at high angles of attack. If the NASA Bisonic Wind tunnel problems cannot be overcome, it is recommended that the measurements be performed in a wind tunnel having better flow quality.

TABLE I

VERTICAL COMPONENT OF MODAL VELOCITY

Position #		Vertical Modal Velocity (ft/sec)
3	Center	+24.2, +49.2, +79.2
3	Front	+37.5, +77.5
3	Back	-7.4, +42.4, +70
6	Back	-2.5, +17.5, +42.5
10	Back	-32.5, -22.5, -2.5
11	Center	-17.5, +17.5
11	Front	-7.5, 7.5, 37.5
11	Back	-27.5, -7.5, 2.5, 17.5
12	Center	-16.5, -11.75
12	Front	-7.5, 7.5, 35
12	Back	-7.5, 7.5, 32.5
13	Front	-7.5, 7.5, 37.5
13	Back	-10, 7.5, 37.5
14	Center	-7.5, 7.5, 42.5
14	Back	-10, 2.5, 22.5
5	Center	42.5, 75.0
5	Front	20, 47.5, 77.5
5	Back	22.5, 47.5
6	Center	47.5, 67.5
6	Front	(2.5), 17.5, 42.5, (72.5)
7	Center	37.5, 67.5
7	Front	-2.5, 17.5, 42.5
7	Back	-2.5, 17.5, (42.5)
10	Center	17.5, 47.5
10	Front	37.5, 52.5
13	Center	-7.5, 7.5, 17.5, 37.5
14	Front	17.5, 42.5

TABLE II

VELOCITY VECTOR IN XY PLANE

Position #	θ, VELOCITY MAGNITUDE
3 Center	4.82°, 288.05; 9.73°, 291.22; 15.43°, 297.76
Front	7.50°, 287.21; 15.22°, 295.11
Back	-1.44°, 293.64; 8.22°, 296.60; 12.41°, 301.78
5 Center	8.32°, 291.07; 14.47°, 297.56
Front	4.02°, 285.35; 9.47°, 288.59; 15.23°, 295.01
Back	4.47°, 288.82; 9.37°, 291.84
6 Center	9.42°, 290.24; 13.26°, 294.18
Front	0.50°, 288.18; 3.48°, 288.70; 8.39°, 291.29; 14.21°, 297.15
Back	-0.50°, 291.44; 3.44°, 291.95; 8.30°, 294.51;
7 Center	7.27°, 296.46; 12.92°, 301.73
Front	-0.50°, 288.38; 3.47°, 288.90; 8.38°, 291.49
Back	-0.50°, 290.41; 3.45°, 290.93; 8.33°, 293.49
10 Center	3.38°, 296.78; 9.11°, 300.04
Front	7.23°, 297.14; 10.07°, 300.39
Back	-6.28°, 297.05; -4.36°, 296.13; -0.49, 295.28
11 Center	-3.41°, 293.84; 3.41°, 293.84
Front	-1.47°, 292.99; 1.47°, 292.99; 7.30°, 295.28
Back	-5.34°, 295.38; -1.46°, 294.20; 0.49°, 294.11; 3.41°, 294.62
12 Center	-3.30°, 291.29; -2.31°, 291.05
Front	-1.48°, 290.56; 1.48°, 290.56; 6.87°, 292.56
Back	-1.49°, 289.07; 1.49°, 289.07; 6.42°, 290.79
13 Center	-1.49°, 288.55; 1.49°, 288.55; 3.47°, 288.98; 7.41°, 290.88
Front	-1.50°, 287.36; 1.50°, 287.36; 7.44°, 289.70
Back	-1.99°, 288.22; 1.49°, 288.15; 7.42°, 290.48
14 Center	-1.48°, 290.61; 1.48°, 290.61; 8.32°, 293.60
Front	3.46°, 290.12; 8.35°, 292.69
Back	-1.97°, 291.33; 0.49°, 291.17; 4.42°, 292.03

$$\theta^* = \tan^{-1} \frac{V_v}{V_H}$$

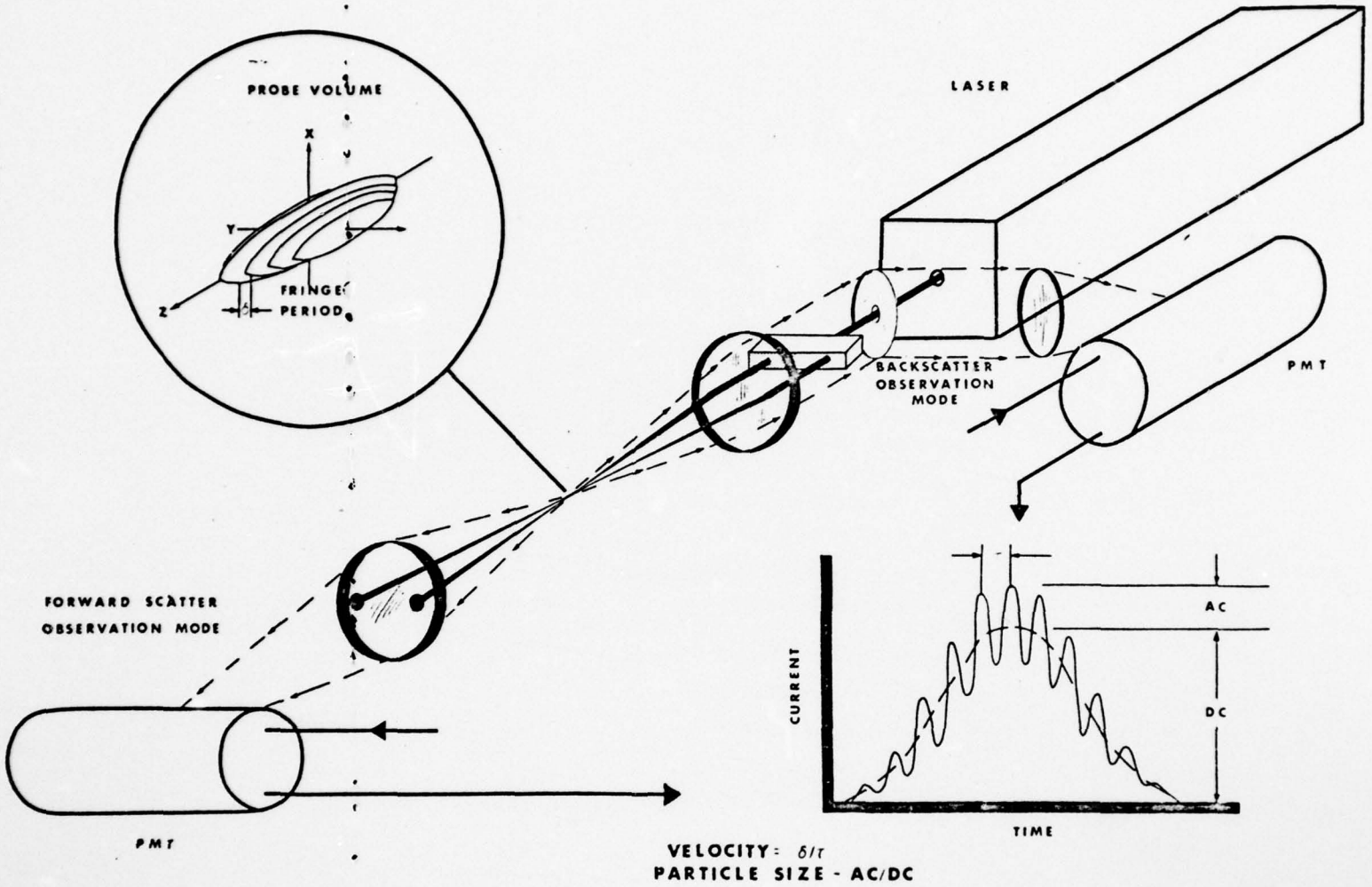

Fig. 1 Standard Interferometer System for Velocity and Particle Size Measurement

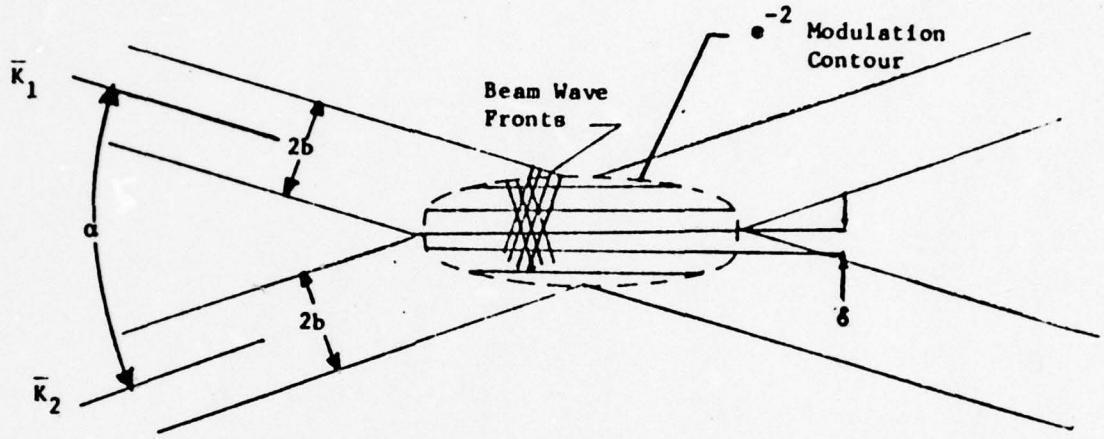

Fig. 2 Huygen's Diagram of Interference Fringe Generation in PM Probe Volume

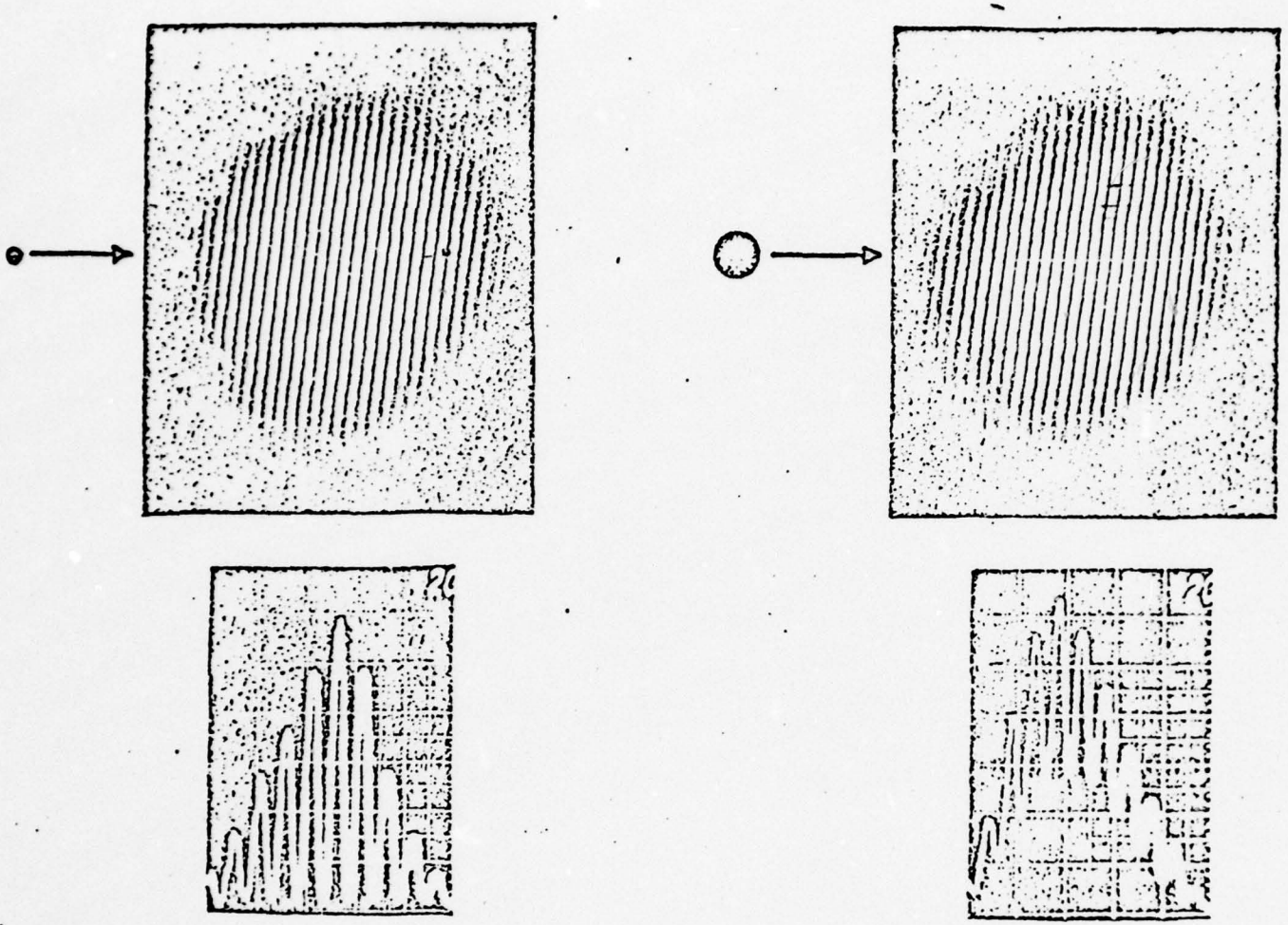

FIG. 3 THE VALUE OF THE AC SIGNAL COMPONENT RELATIVE TO THE AVERAGE SIGNAL COMPONENT DEPENDS ON PARTICLE SIZE.

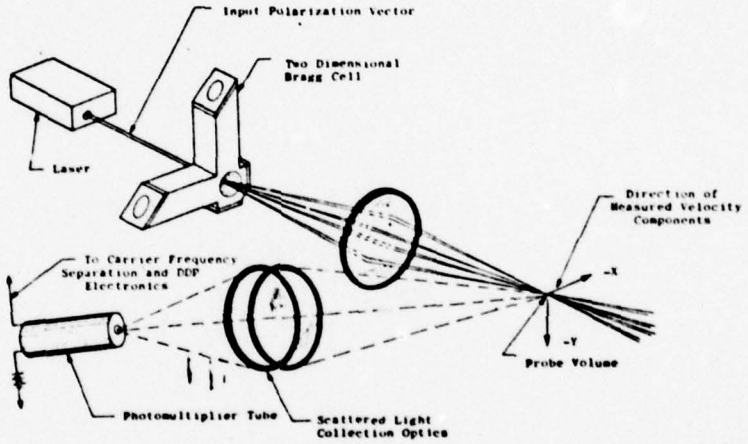

Fig. 4 Schematic of a LDV system using a two-dimensional Bragg cell.

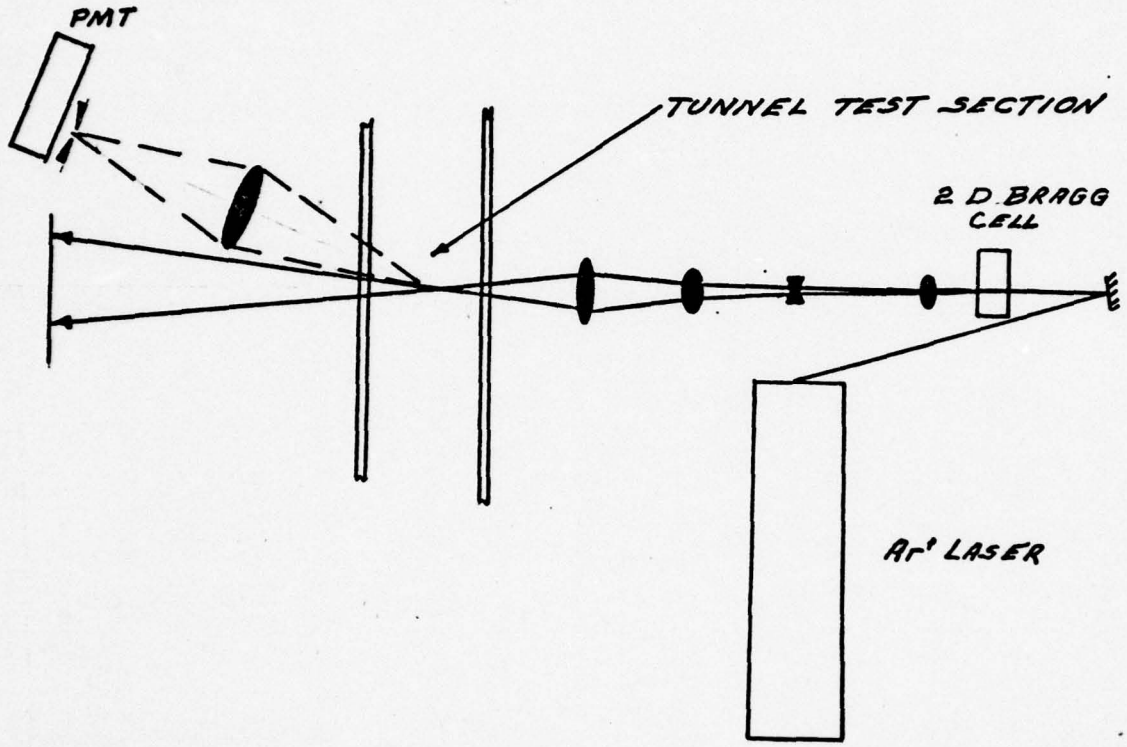

Fig. 5 Schematic diagram of LV system used in NASA/Marshall 7" x 7" Bisonic Wind Tunnel.

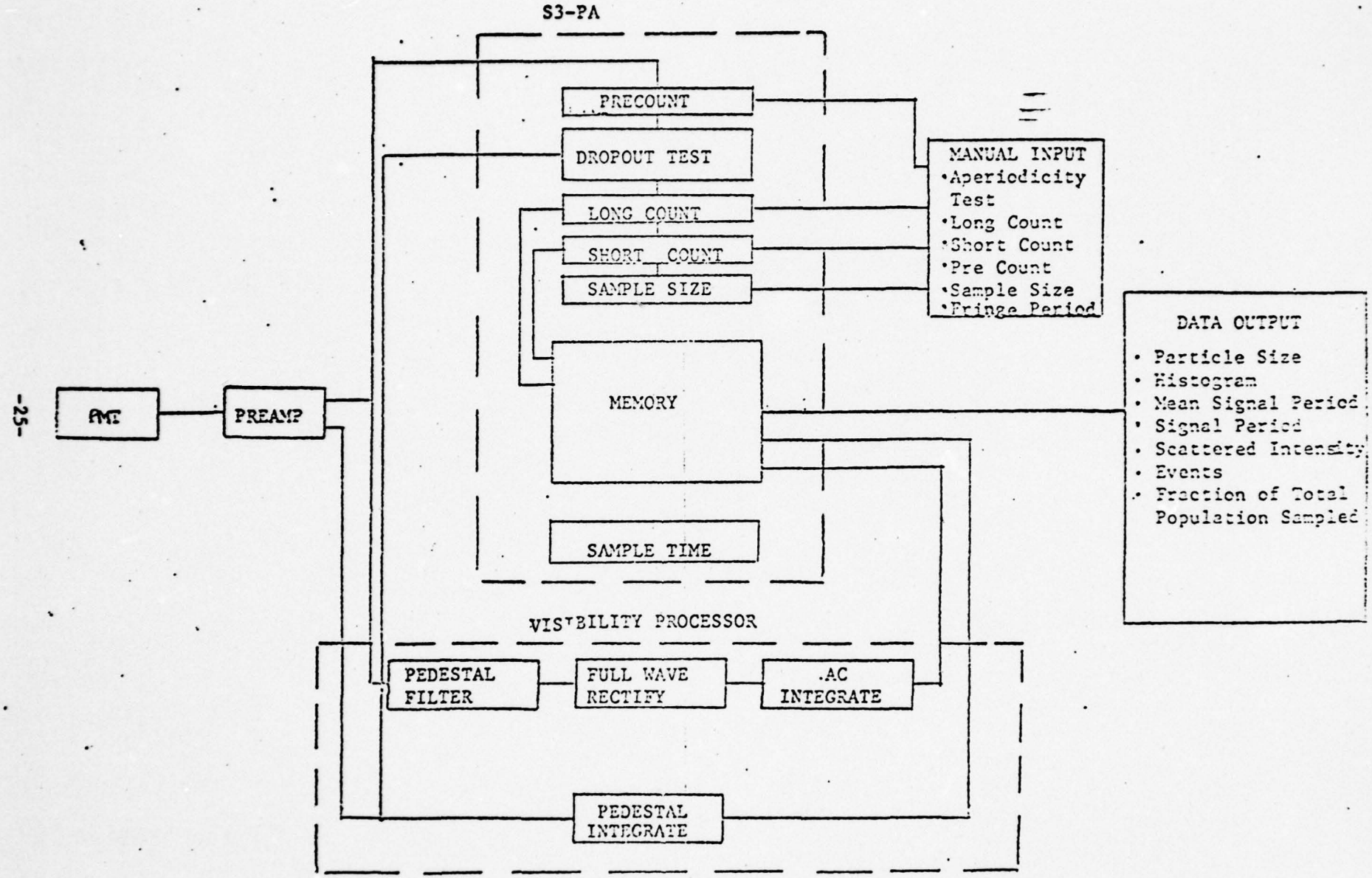

Fig. 6 Schematic diagram of LV Signal Processing System

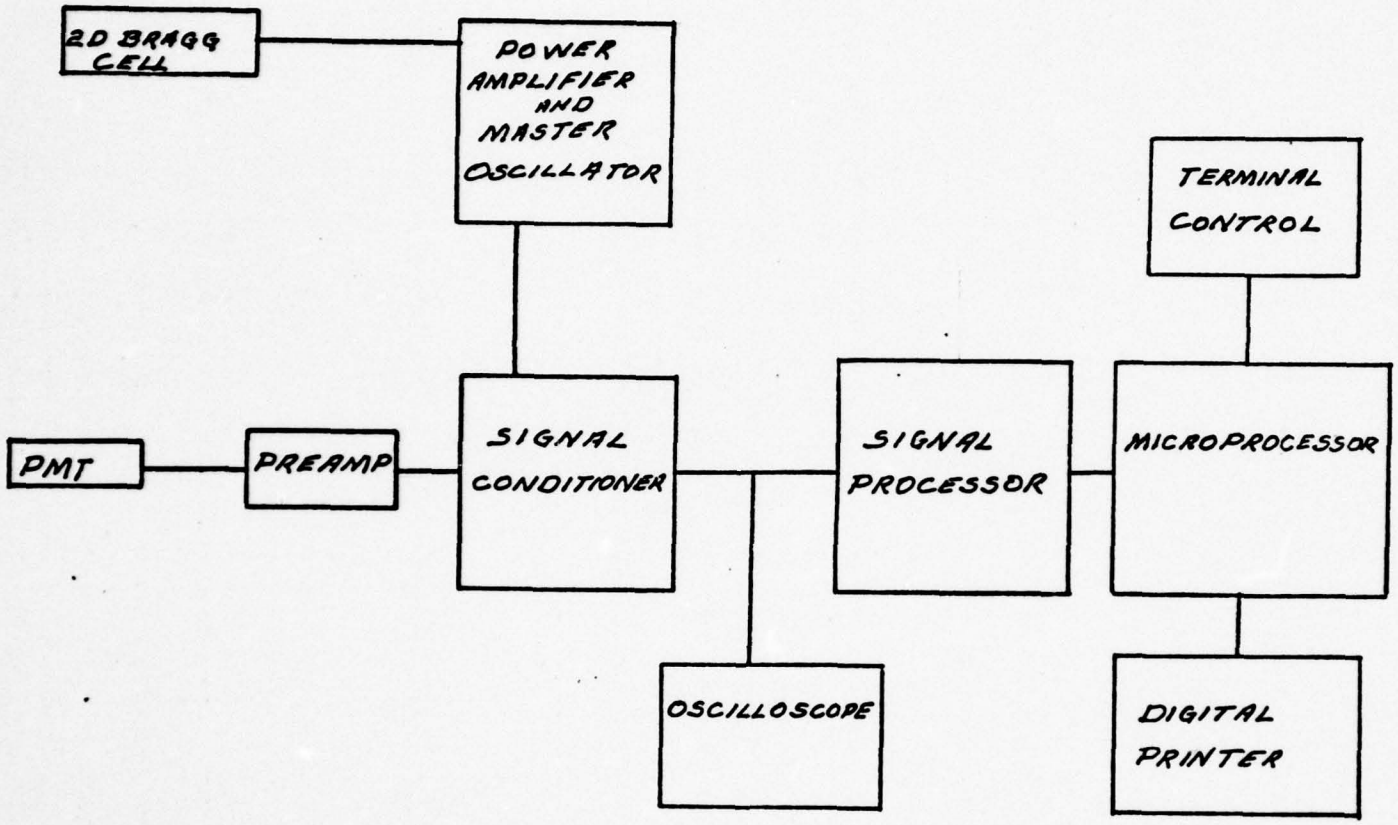

Fig. 7 Schematic diagram of LV signal processing and data acquisition systems used in the NASA tests.

LONG COUNT =00016
SHORT COUNT =00310
PREDOUNT =00383
NUMBER OF READINGS INTO MEMORY =00900
MAX APERIODICITY (K) = 5.000000
FRINGE PERIOD = 167.4000
HIGH PASS FILTER SETTING (MHZ) = 2.000000

POSITION 5 BACK HORIZONTAL VELOCITY
COMPONENT 100 ft/sec VELOCITY OFFSET

388.6389 4.125106 4.567304 04576

388.8839 3.613228 5.828152 00638

388.4818 3.715824 5.000671 04648

387.6513 3.768751 5.504822 03535

302.6206
380.2145
397.7822
387.5490
395.1738
387.5498
380.2145
387.5498
400.4253
387.5498
380.2145
392.5994
395.1738
370.8554
382.6206
380.2145
395.1738
397.7822
387.5498
387.5490
387.5498
403.1837
382.6206
397.7822
392.5994
392.5994
395.1738
377.8307
392.5994
335.7326
345.3524
395.1738
382.6206
366.3465
395.1738
397.7822
397.7822

Fig. 8 Typical data output example.

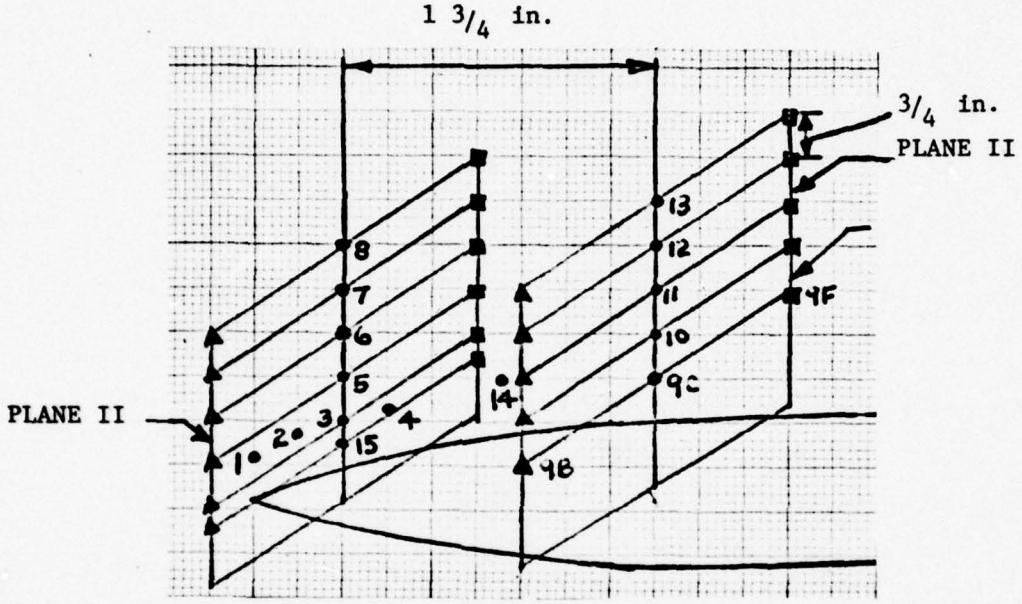

● Circles = Centerline positions (labeled with c,e.g. 9C).

▲ Back positions (labeled with B,e.g., 9B).

■ Forward positions (labeled with F,e.g., 9F)

Fig. 9 Location of measurement points relative to model.

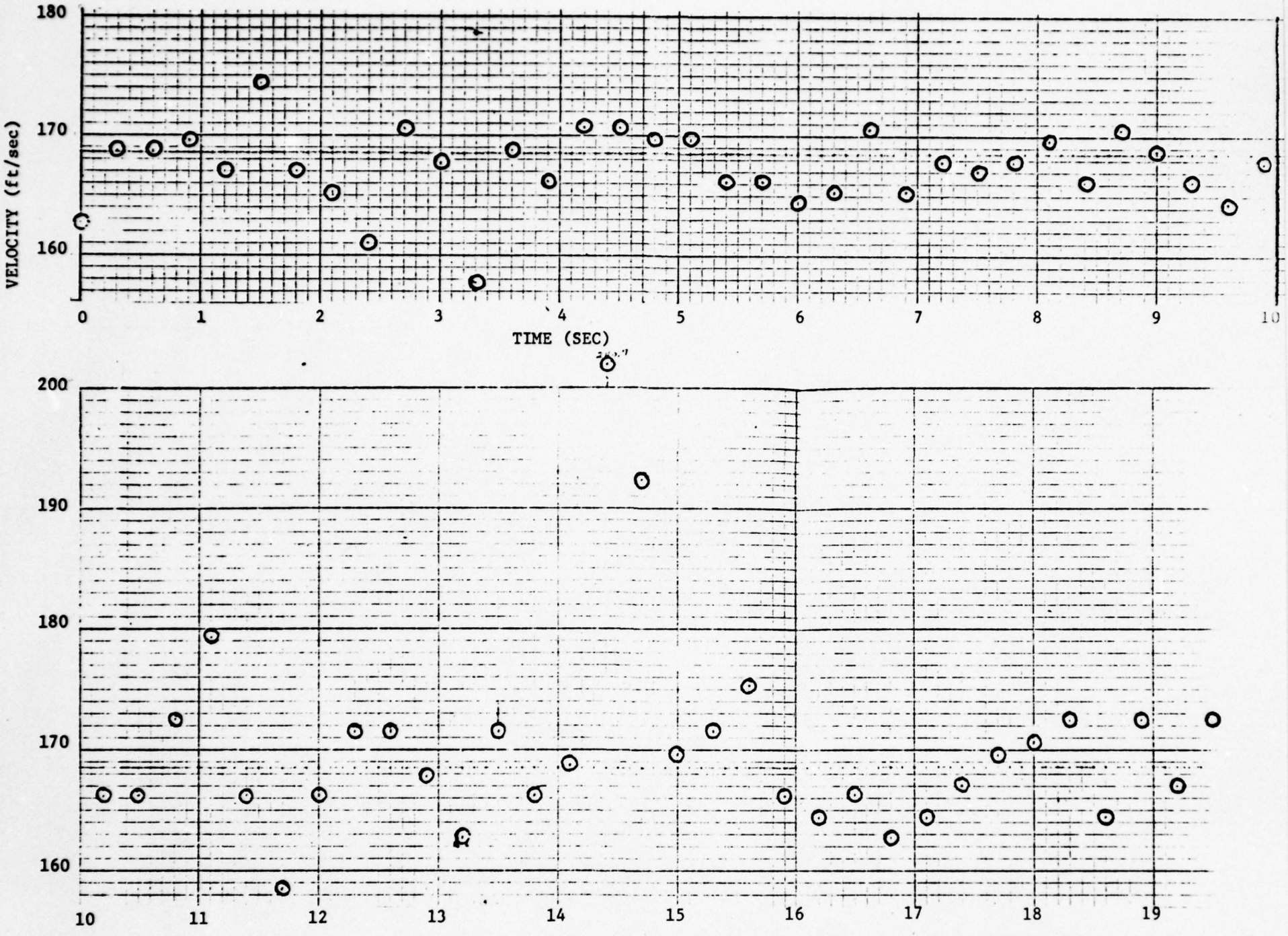

Fig. 10 Long term variation of wind tunnel velocity

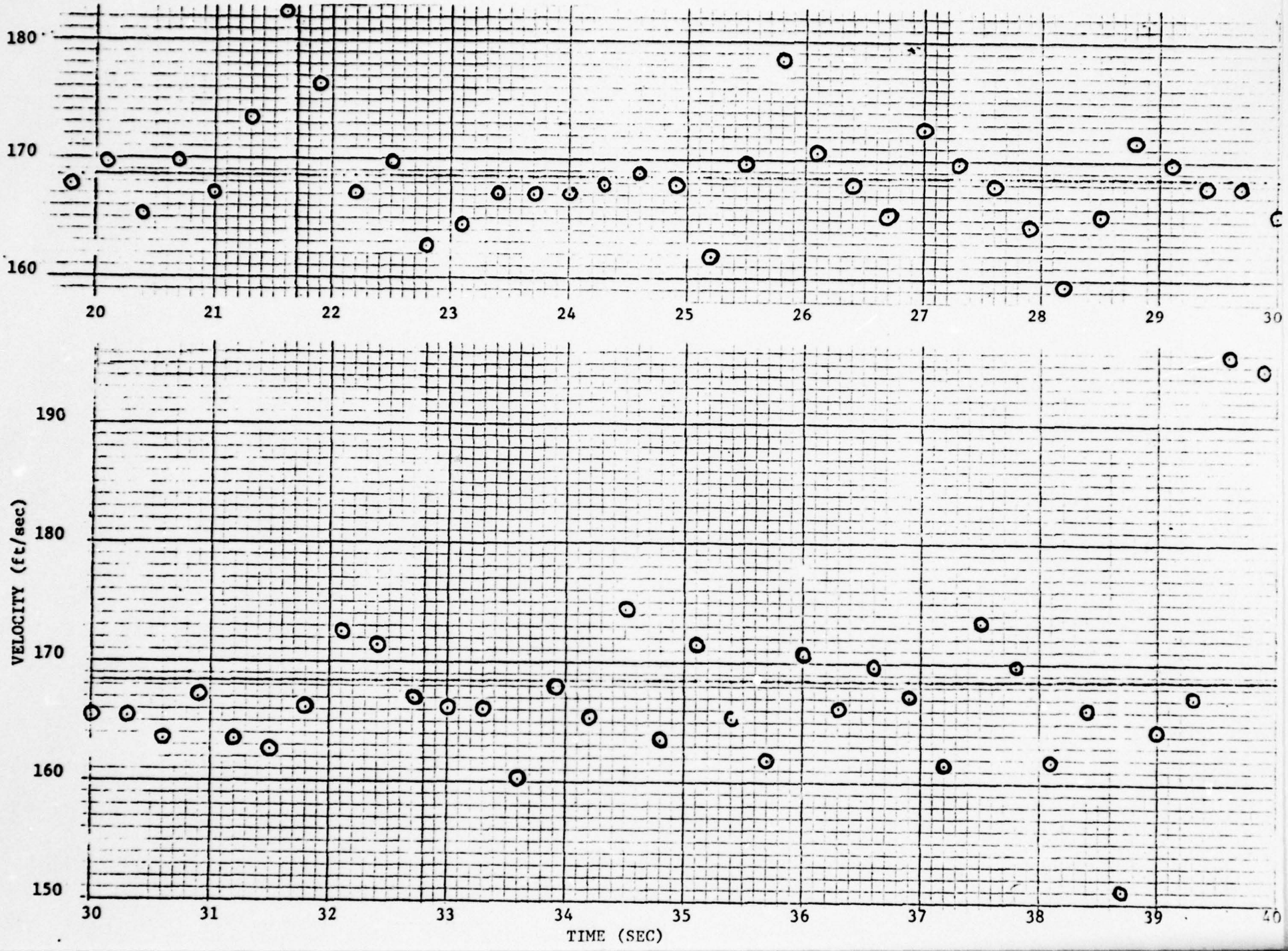
180
170
160
20
21
22
23
24
25
26
27
28
29
30
190
180
170
160
150
VELOCITY (ft/sec)
30
31
32
33
34
35
36
37
38
39
40
TIME (SEC)

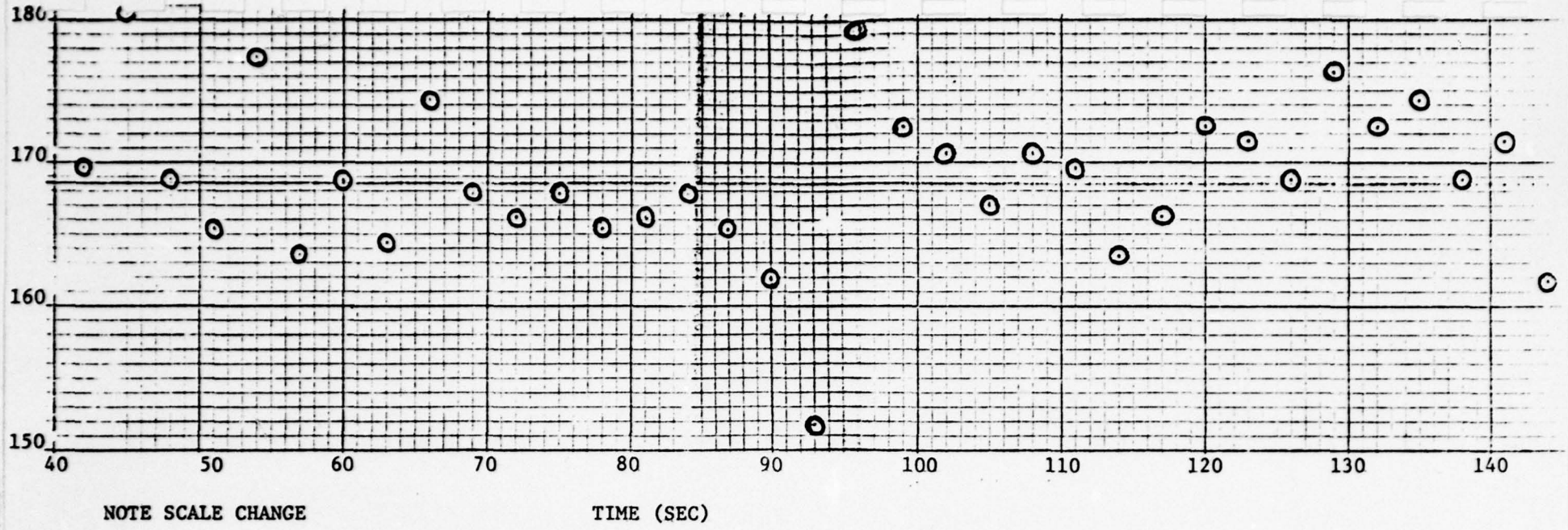
180
170
160
150
40
50
60
70
80
90
100
110
120
130
140
NOTE SCALE CHANGE
TIME (SEC)

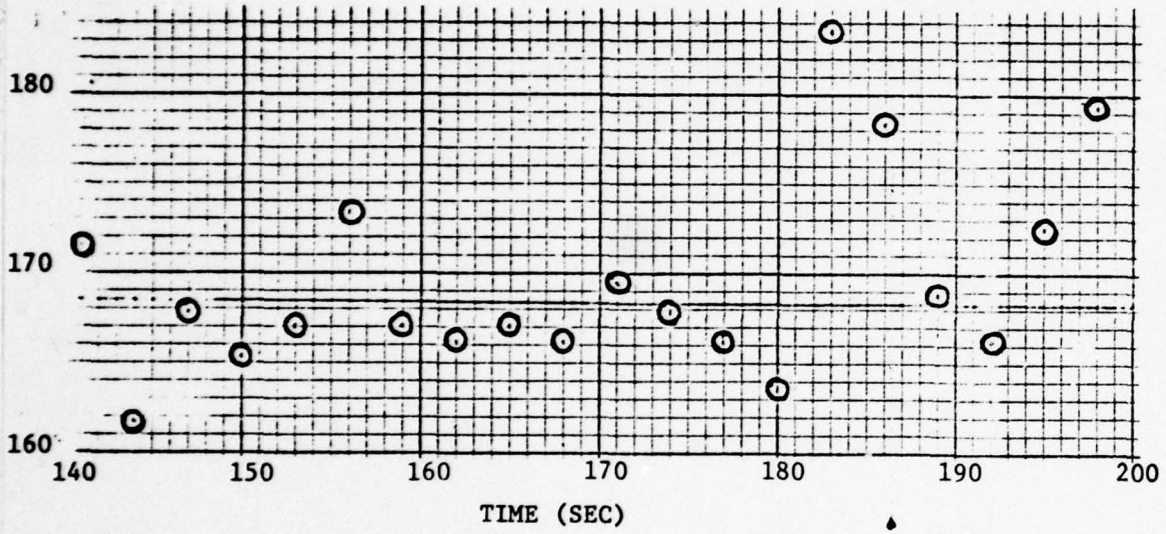
180
170
160
140
150
160
170
180
190
200
TIME (SEC)

Fig. 10 (cont.)

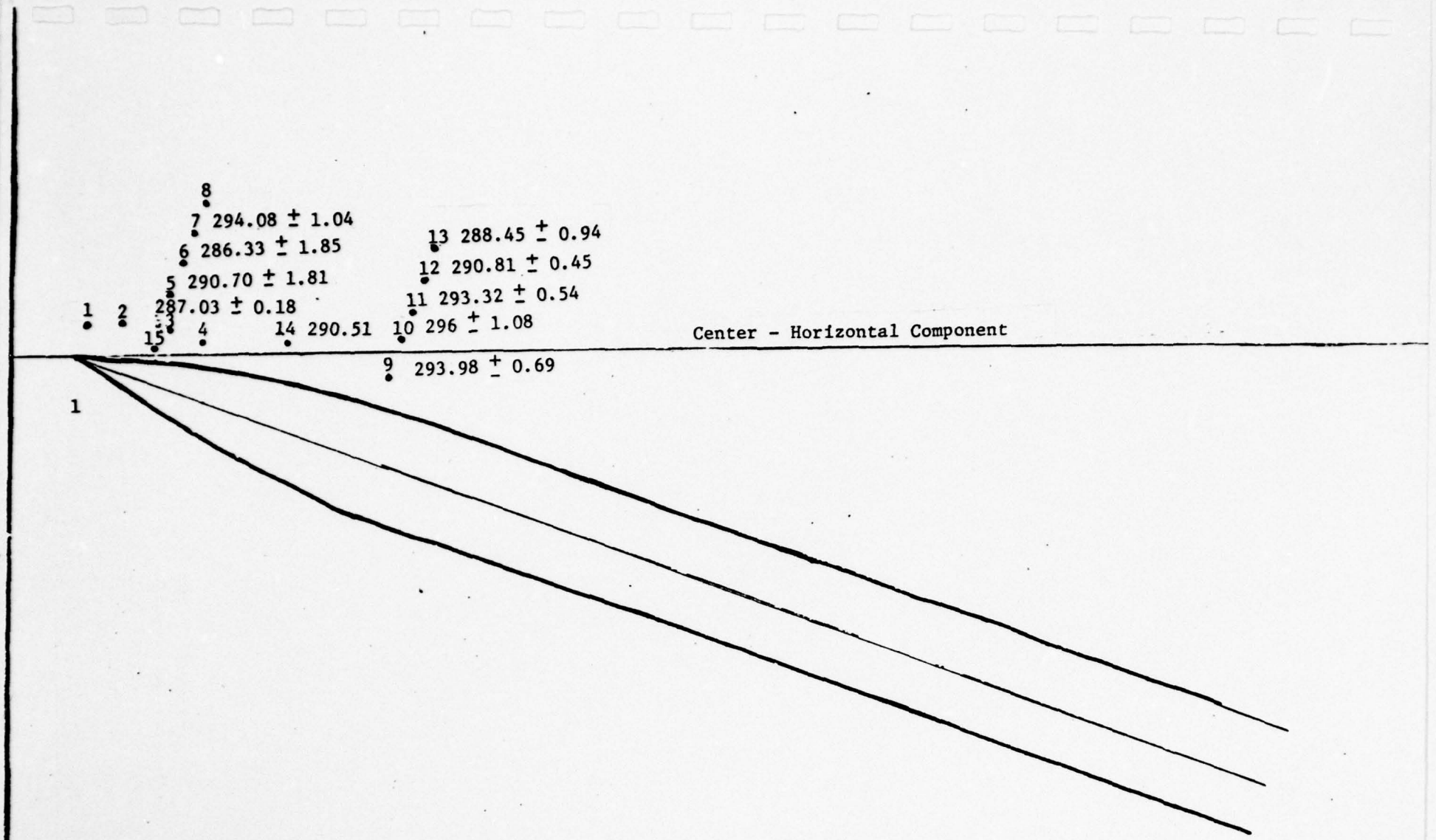

Fig. 11 Mean horizontal velocity components on the center plane.

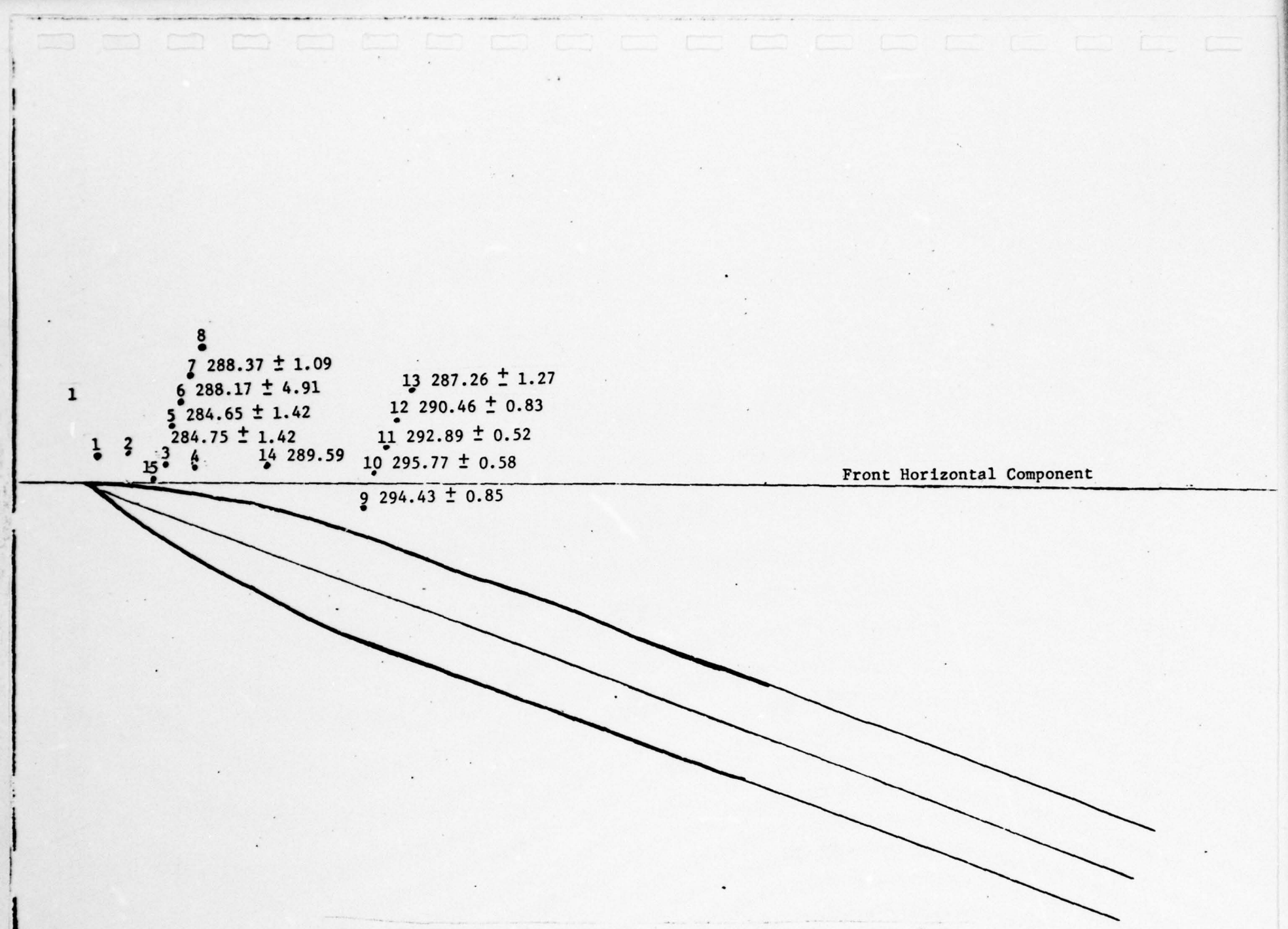

Fig. 12 Mean horizontal velocity components on the center plane.

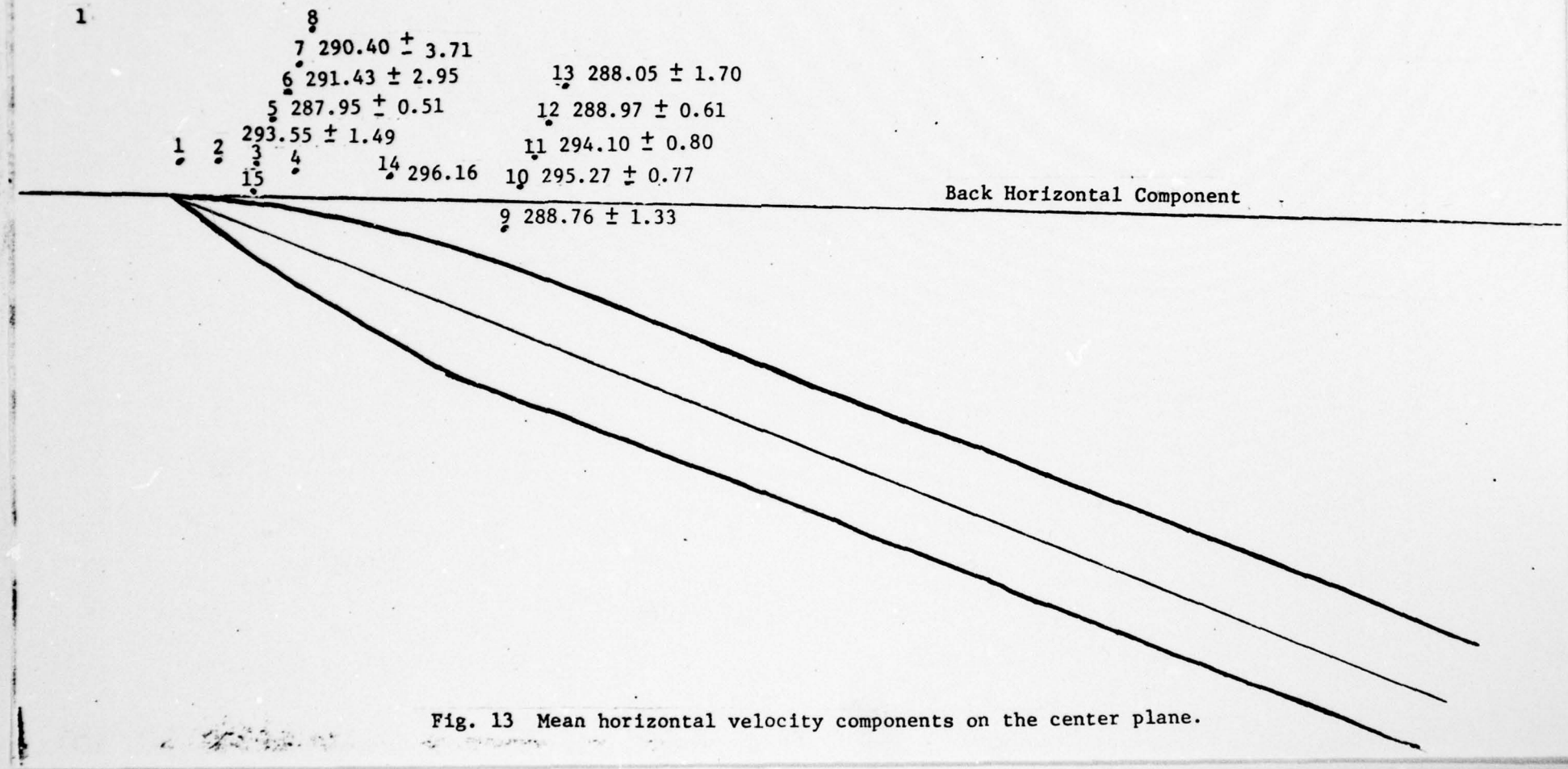

Fig. 13 Mean horizontal velocity components on the center plane.

Fig. 14 Histogram of the vertical velocity component at Position 3, Back.

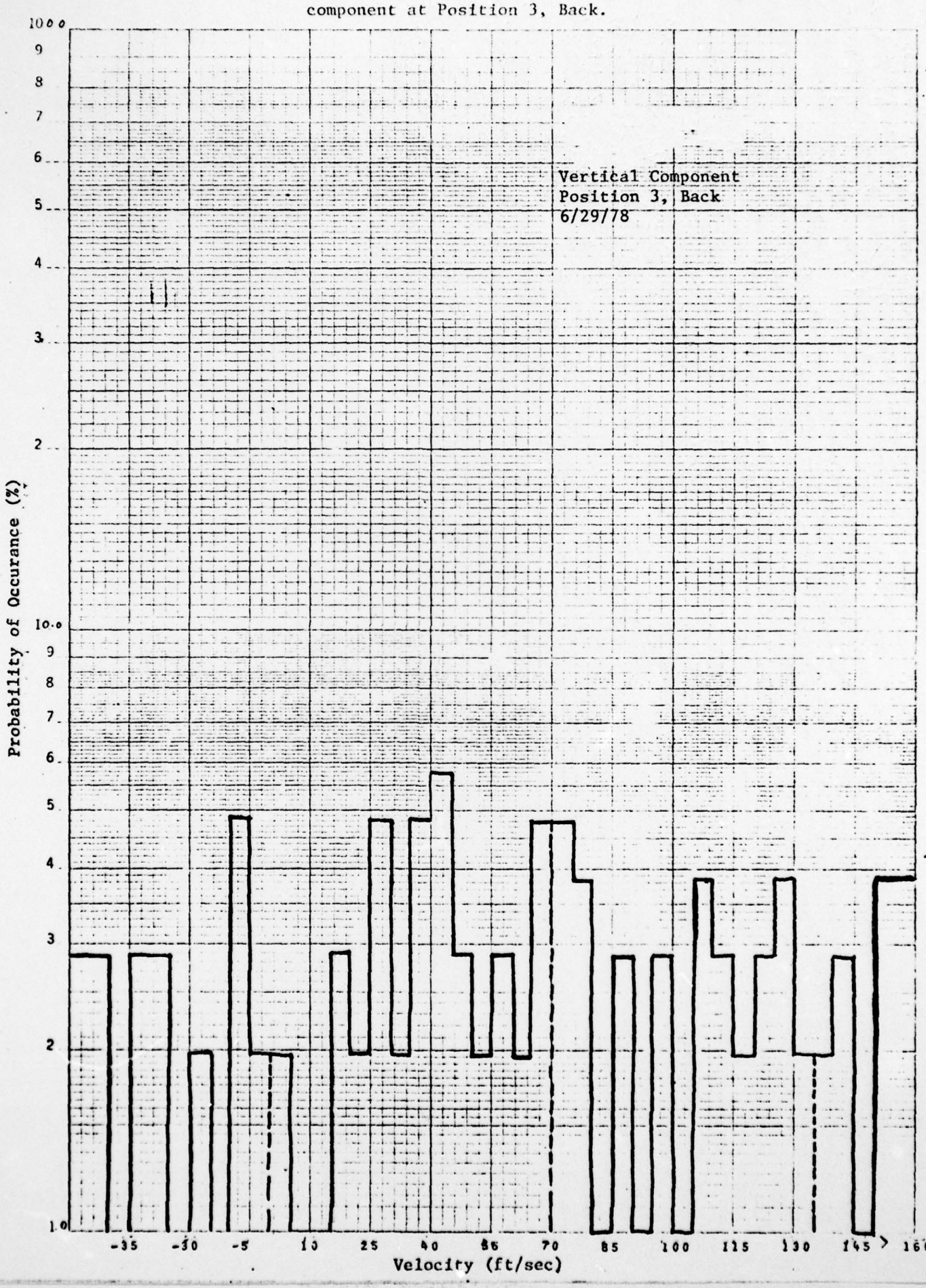

Fig. 15 Histogram of the vertical velocity component at Position 3, Center.

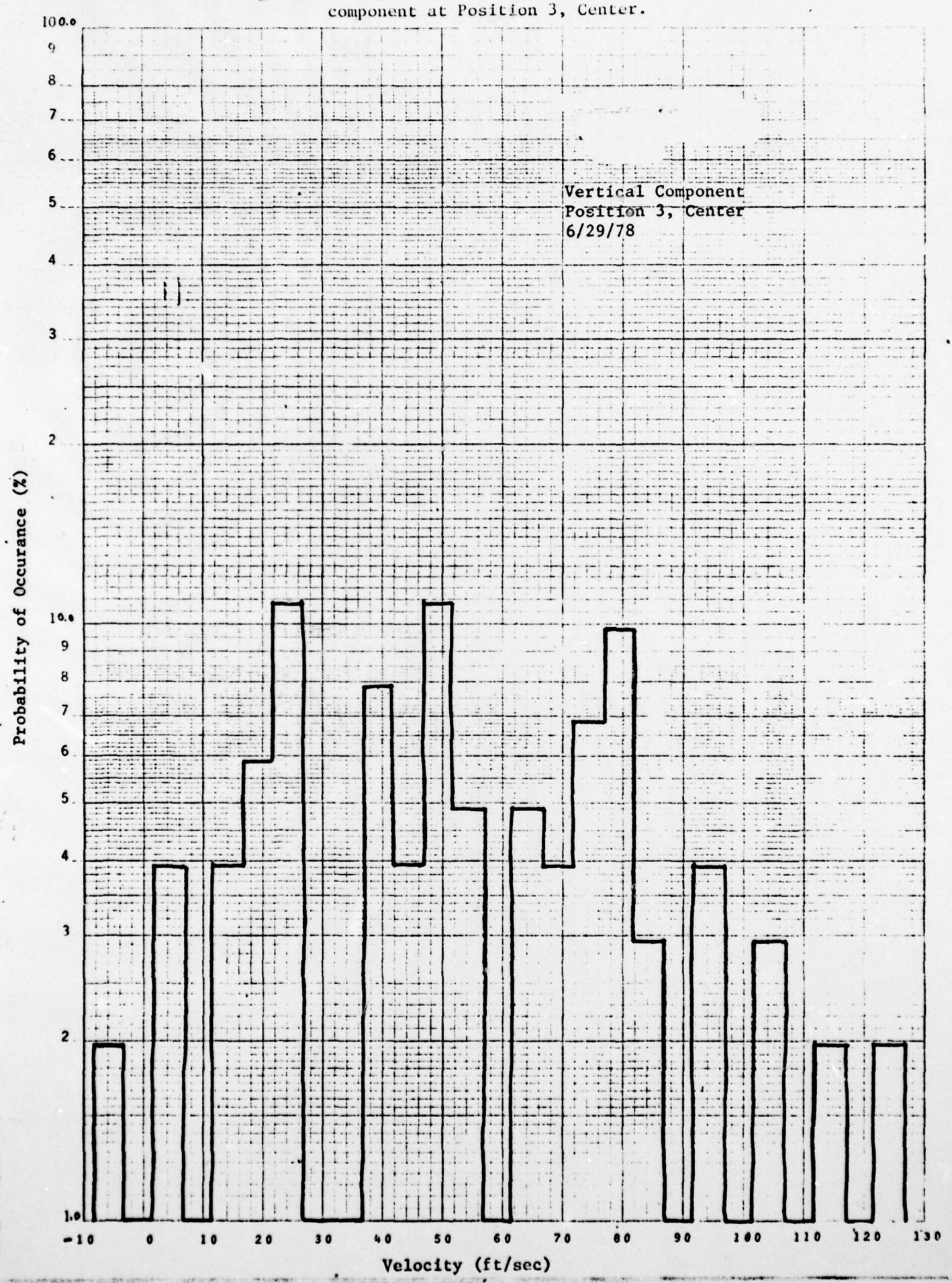

Fig. 16 Histogram of the vertical velocity component at Position 3, Front.

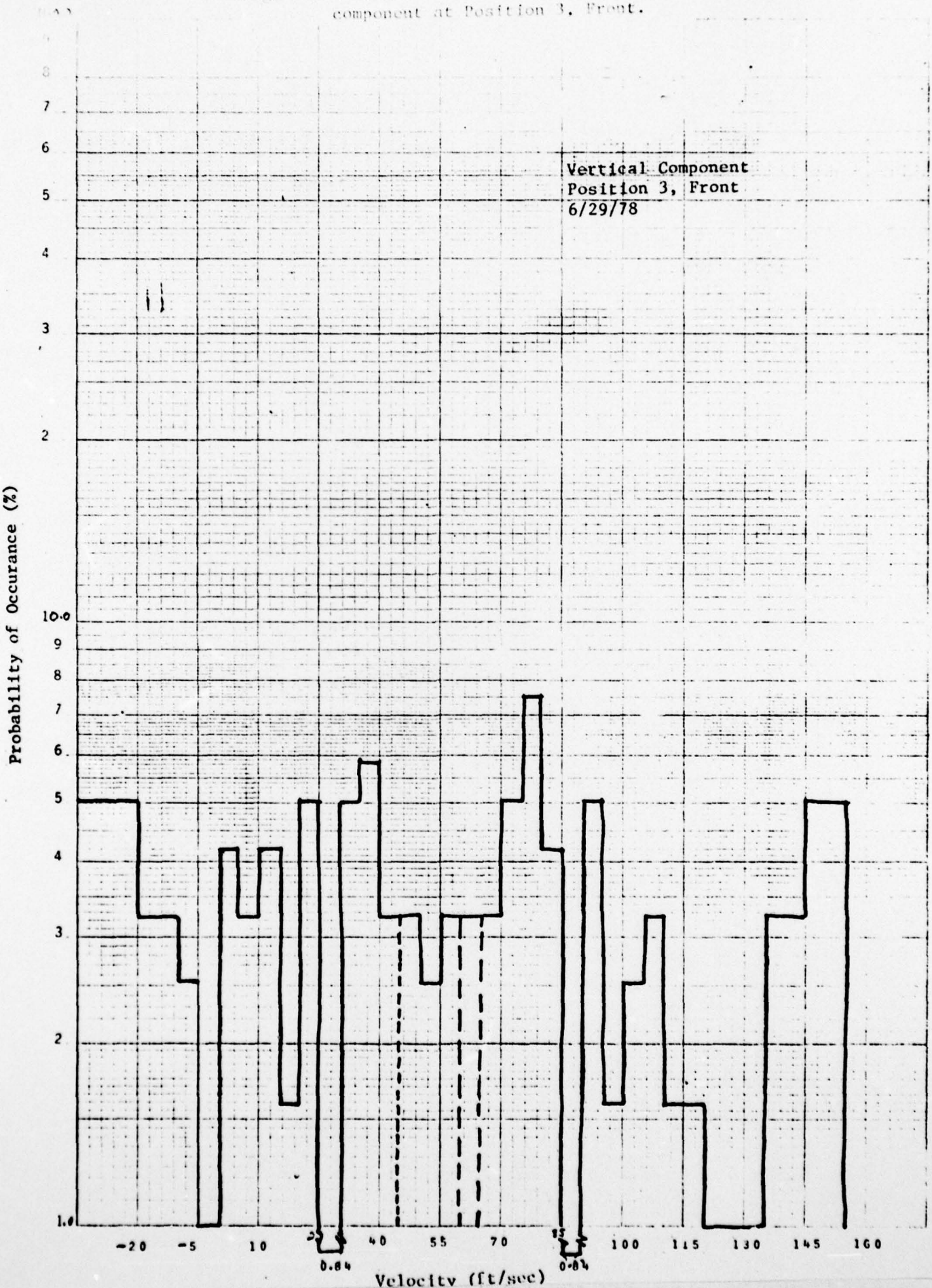

Fig. 17 Histogram of the vertical velocity component at Position 11, Back.

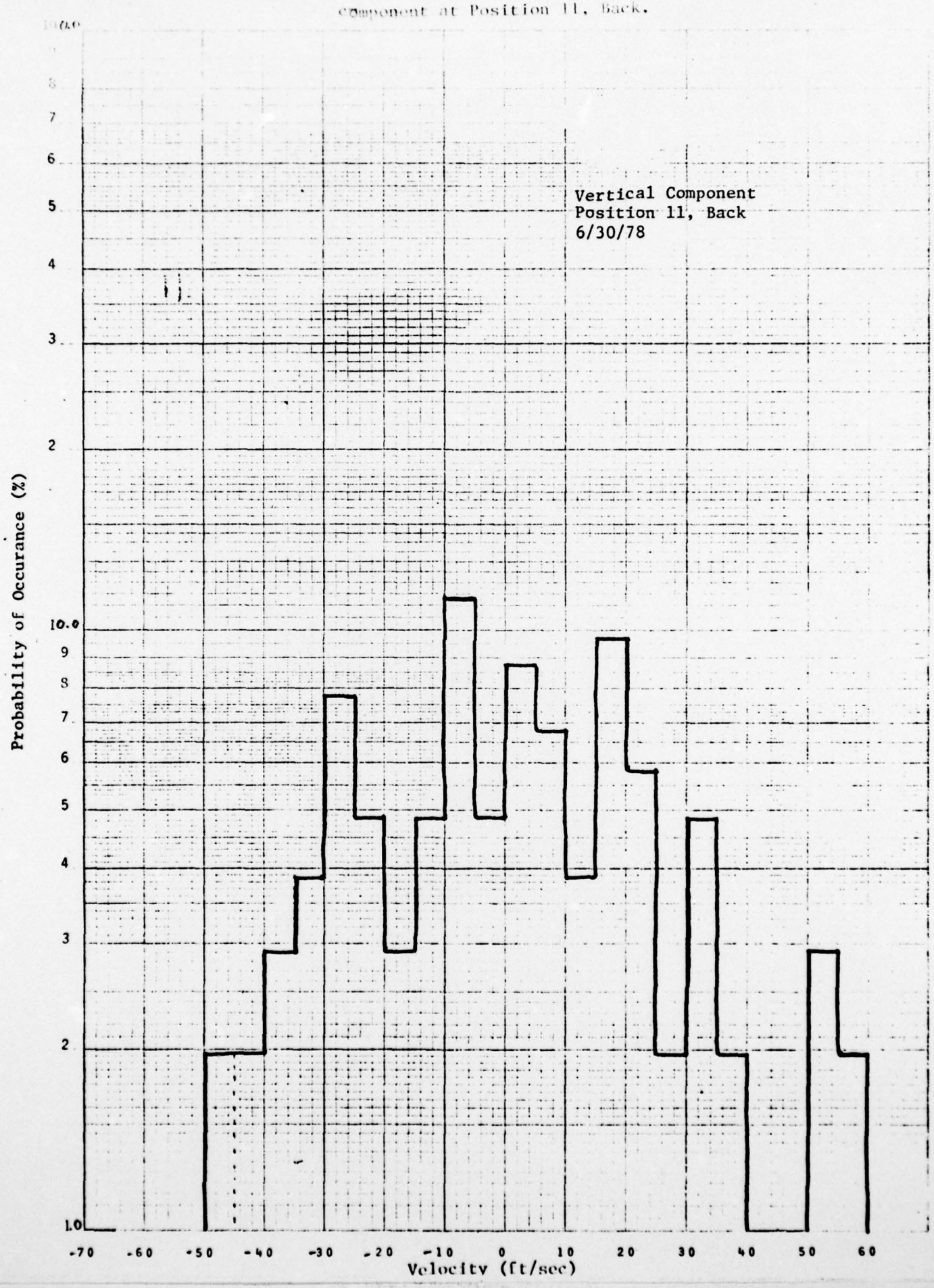

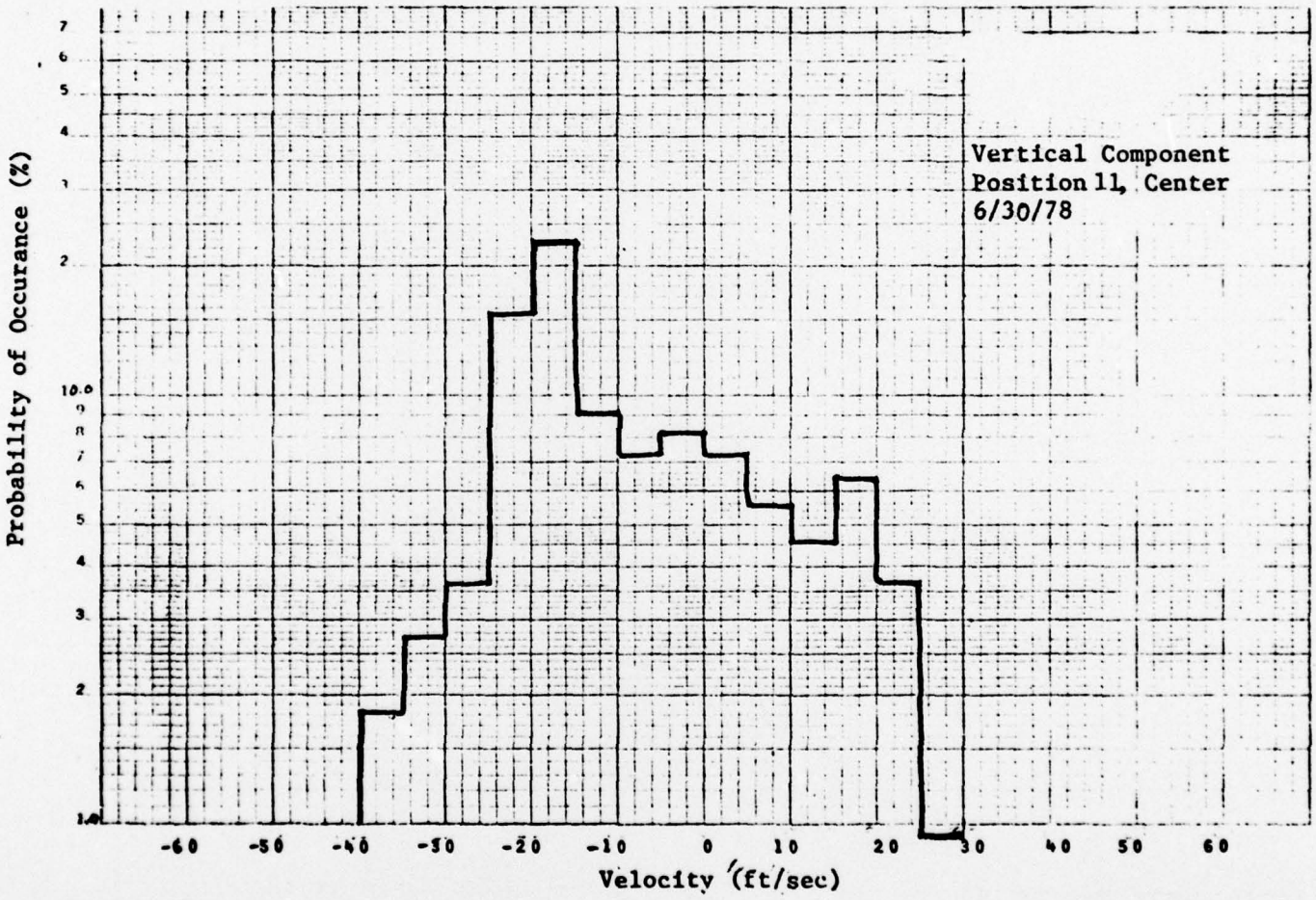

Fig. 18 Histogram of the vertical velocity component at Position 11, Center.

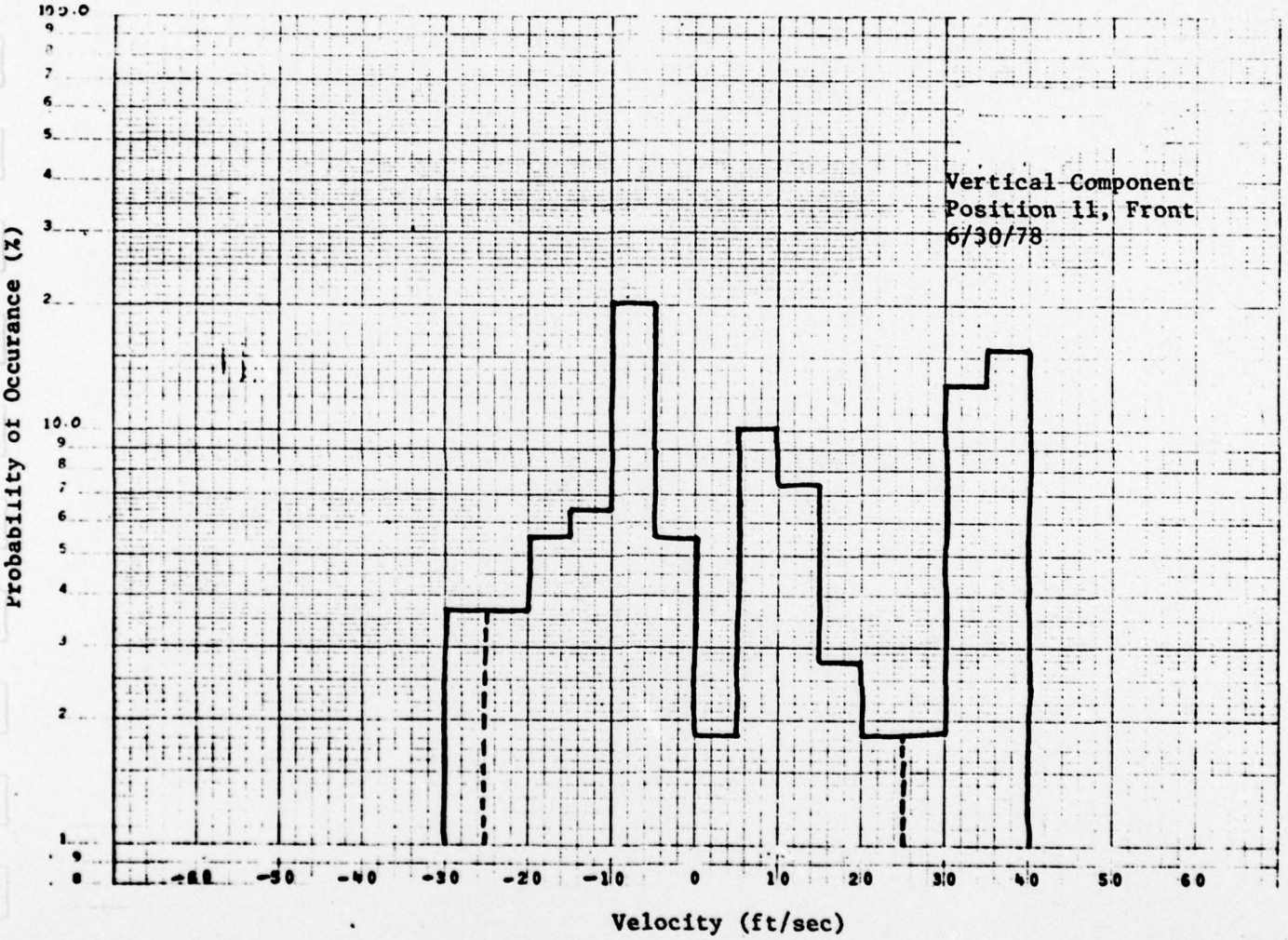

Fig. 19 Histogram of the vertical velocity component at Position 11, Front.

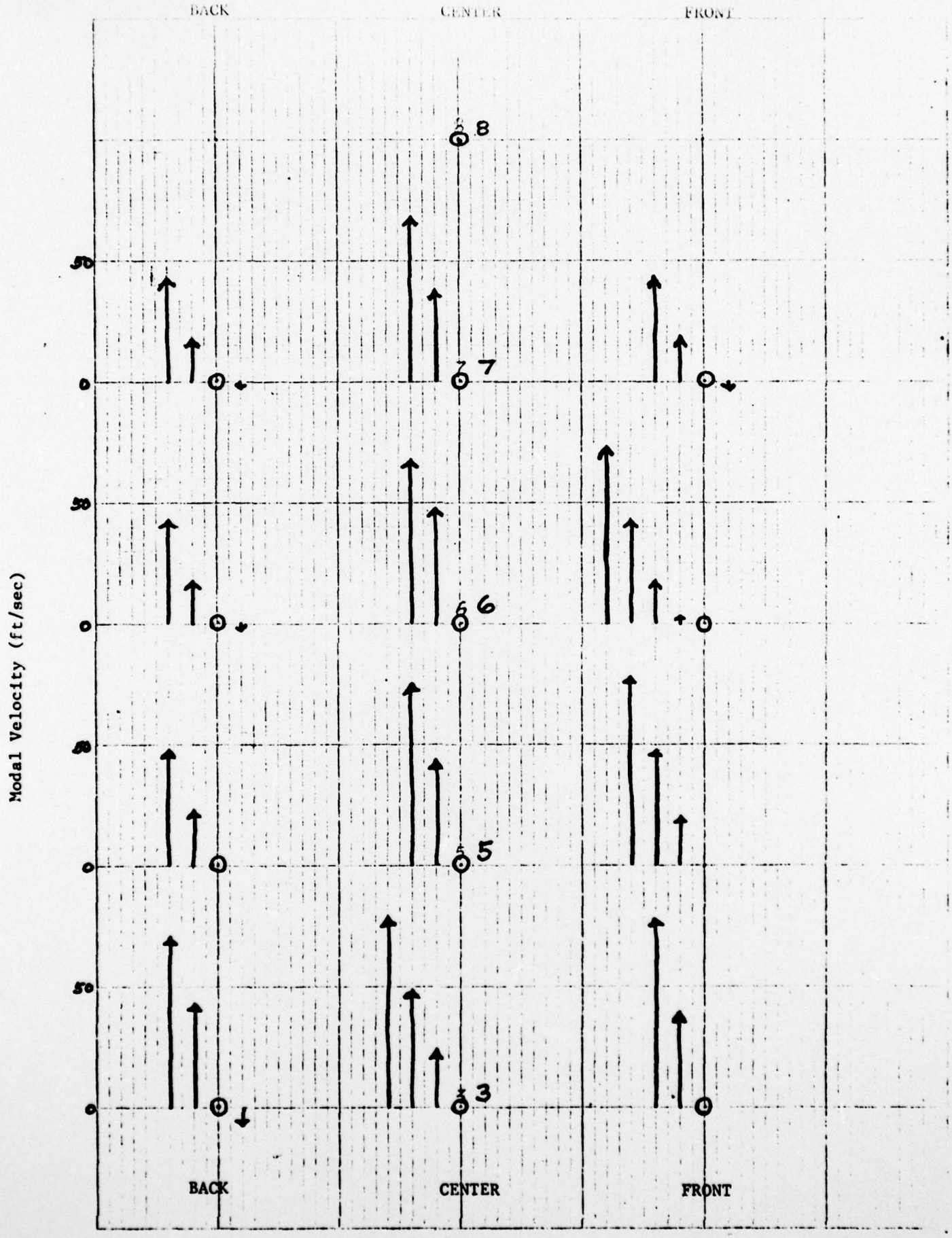

Fig. 20 Vertical velocity components in Plane I.

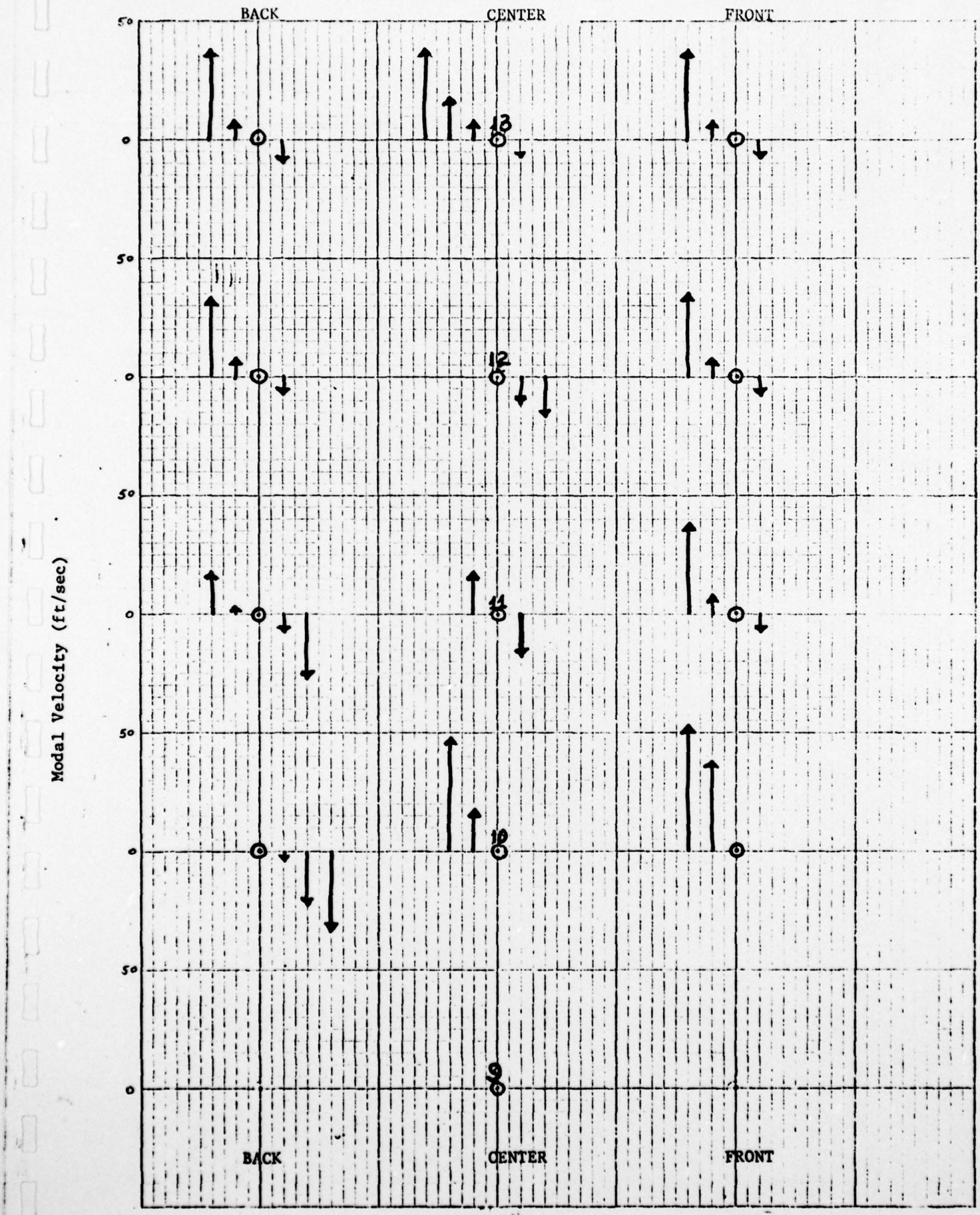

Fig. 21 Vertical velocity components in Plane II.

Fig. 22 Schematic representation of velocity vector in Back Plane.

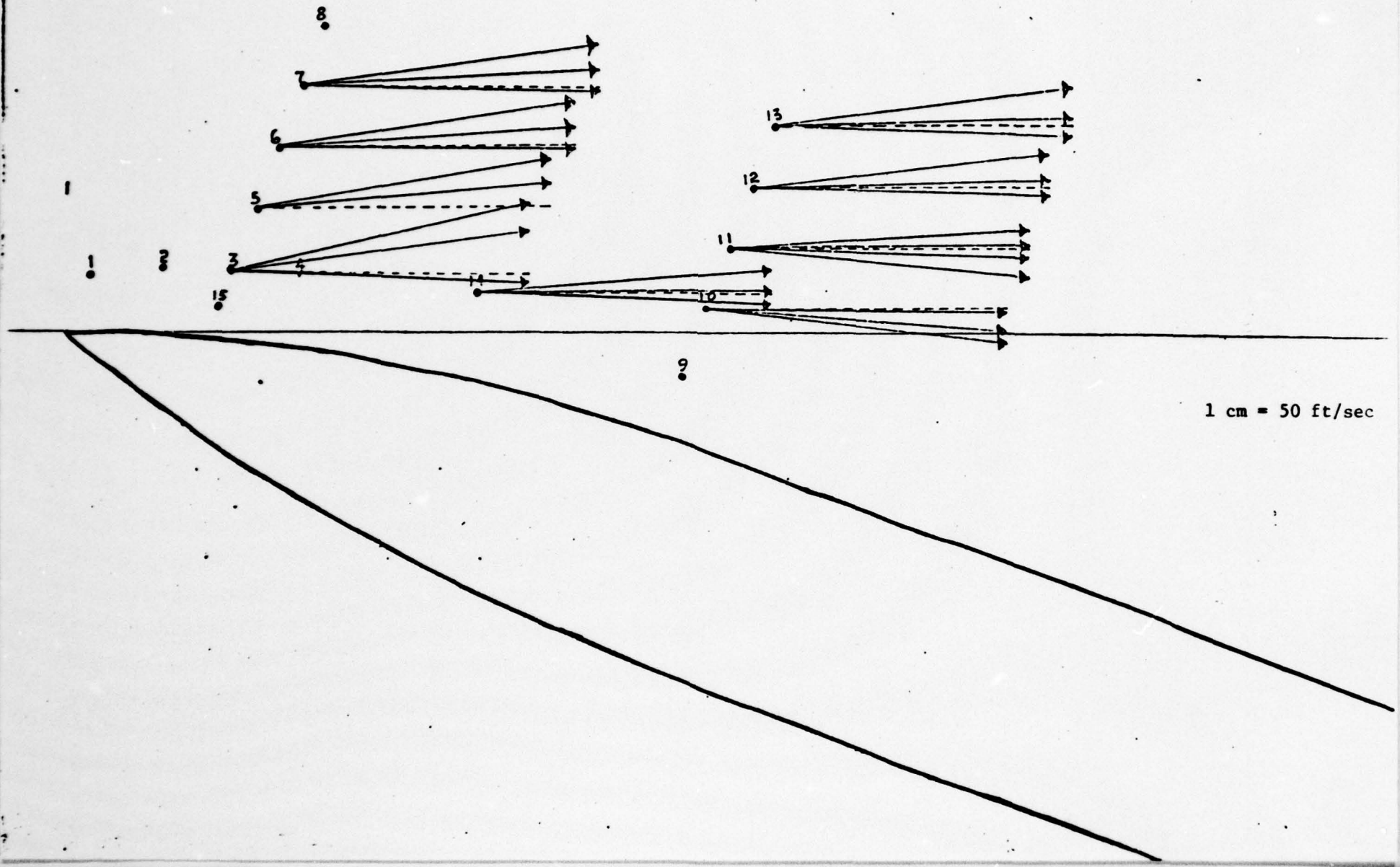

Fig. 23 Schematic representation of velocity vector in Center Plane.

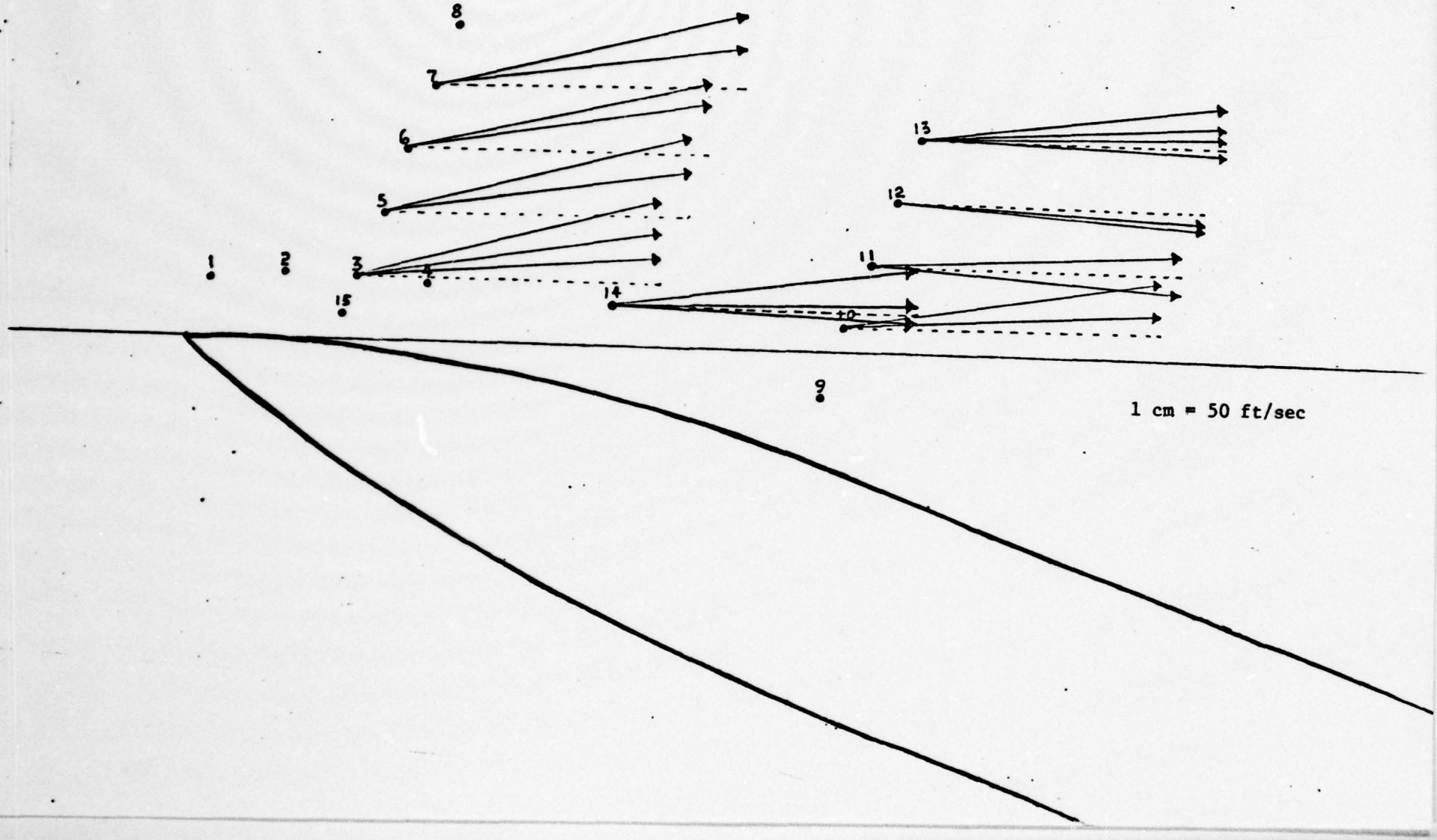

Fig. 24 Schematic representation of velocity vector in Forward Plane.

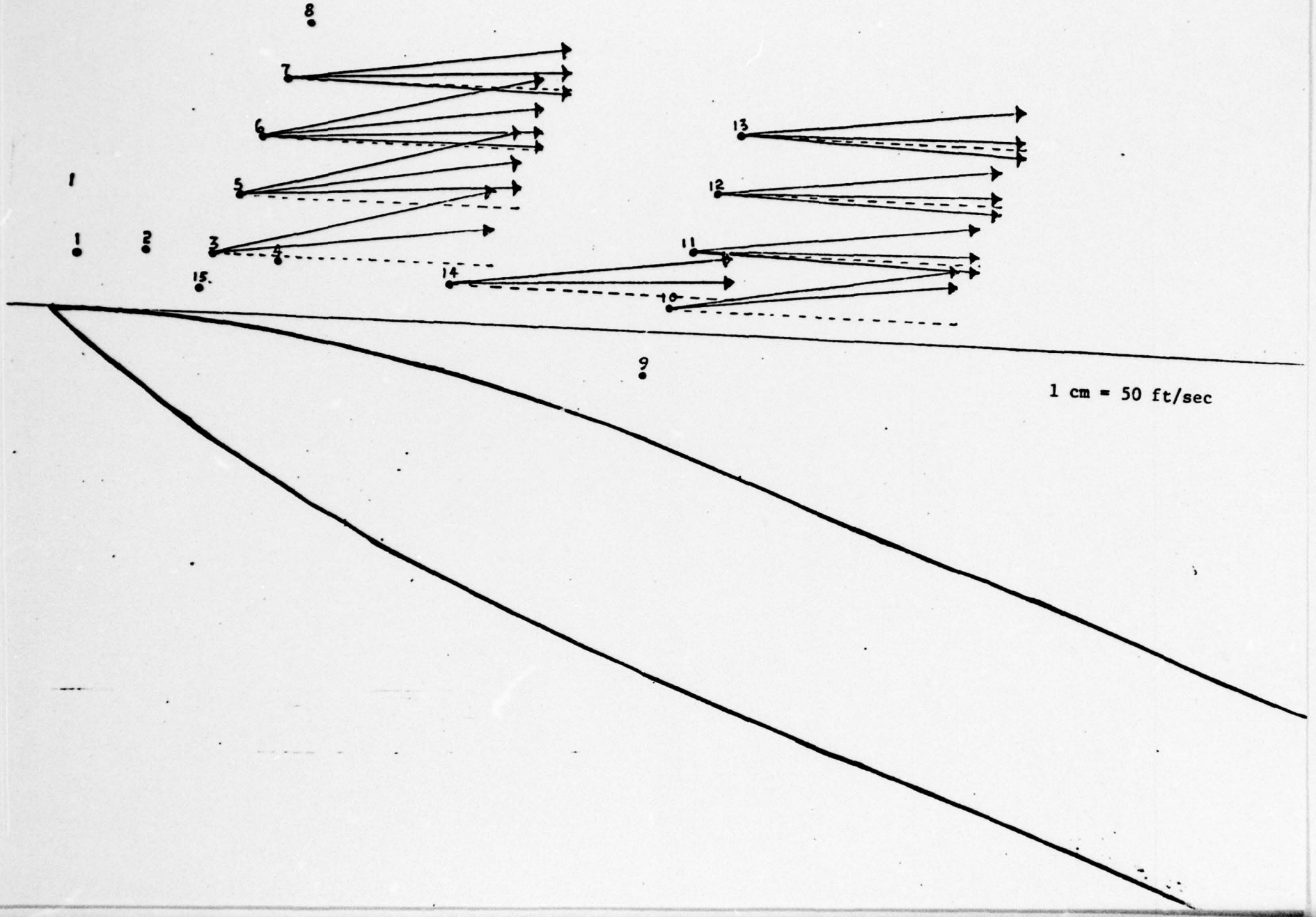

REFERENCES

1. Farmer, W. M. and Hornkohl, J. O., "Two-Component, Self-Aligning Laser Vector Velocimeter," Applied Optics, Vol. 12, pages 2636-2640, November 1973.